8-7-2018

Effect of Monoethanolamine on the Lipid Metabolism of Prostate Cancer Cells

Jennifer McFaline-Figueroa

EFFECT OF MONOETHANOLAMINE ON THE LIPID METABOLISM OF PROSTATE CANCER CELLS

by

JENNIFER MCFALINE-FIGUEROA

Under the Direction of Ritu Aneja, PhD

ABSTRACT

The ability of cancer cells to synthesize and store lipids in the form of lipid droplets (LDs) gives them a proliferative advantage over normal cells. Here, we elucidate the effect of monoethanolamine (Etn) on the lipid metabolism of LD-rich prostate carcinoma (PC3) cells. Etn is a ubiquitous molecule that serves as a phospholipid precursor and has been shown to have anticancer activity, although its mechanism of action is not fully understood. PC3 cells were treated with Etn and evaluated with a combination of biochemical and cell biology techniques. Treatment with Etn caused a decrease in cytosolic LD abundance induced by Ca^{2+}-stimulated lipolysis. Our study effectively implicates the disruption of lipid metabolism as a contributor to Etn-induced cell death. This finding opens new avenues for the development of LD-targeted anticancer therapy.

INDEX WORDS: monoethanolamine, prostate cancer, lipid metabolism, lipid droplets, calcium

EFFECT OF MONOETHANOLAMINE ON THE LIPID METABOLISM OF PROSTATE CANCER CELLS

by

JENNIFER MCFALINE-FIGUEROA

A Thesis Submitted in Partial Fulfillment of the Requirements for the Degree of

Master of Science

in the College of Arts and Sciences

Georgia State University

2018

EFFECT OF MONOETHANOLAMINE ON THE LIPID METABOLISM OF PROSTATE CANCER CELLS

by

JENNIFER MCFALINE-FIGUEROA

Committee Chair: Ritu Aneja

Committee: Vincent Rehder

Liana Artinian

Electronic Version Approved:

Office of Graduate Studies

College of Arts and Sciences

Georgia State University

August 2018

DEDICATION

For my family, and their well-practiced ability not to freak out when I tell them of my life choices, last minute.

Los amo a todos.

ACKNOWLEDGEMENTS

I would be remiss to think that my experience at Georgia State has been an isolated journey. Before I get bogged down mentioning all the people who have been critical in my graduate school career, I would like to extend my thanks to the whole Biology department at GSU. From the professors, to the administrators, to the maintenance people, you all made sure that this experience was the best I could possibly have, and for that I am eternally grateful.

First and foremost, I would like to thank my PI and my thesis committee for all of their support. I appreciate Dr. Aneja for taking me on as a graduate student and allowing me to work in her lab. To my committee members Dr. Rehder and Dr. Artinian for all of their help, guidance and encouragement as I undertook this project. Dr. Artinian and I met during the Summer semester when I was TA'ing a course for Dr. Aneja, and it led to the most wonderful collaboration that turned into my thesis project. Her energy and passion for science and her belief that there is always an experiment to be done inspires me to be a better researcher. Through her, I met Dr. Rehder, who has been, from the moment I met him, a knowledgeable, honest voice of reason, reminding me to always look at the big picture. As a committee, the three always made sure that I was clear on what my goals were, to examine my data with a critical eye, and to ask myself the "what", "where" and "why" before I drew any conclusion.

In this journey, I am often reminded of the people who helped me get here, and the places where I learned how to be a good scientist. I would like to thank my undergraduate institution, University of Puerto Rico- Mayaguez, along with my PI, Dr. Juan Lopez-Garriga and my graduate mentor, Elddie. You were the first to ignite my passion for research, and you remain, to this day, steadfast supporters of my career. I would also like to thank my PI at Georgia Tech, Dr. Johnna

Temenoff and all my T-Lab buds, for helping me expand my scientific interests, granting me every opportunity to grow as a researcher, and for simply being my friends.

I would like to thank my lab members and other science friends I have made at GSU, in particular Ahmed, Nikita, Kimberly, Amanda, Barielba and Felipe. Our goals are vastly different from each other, but I am grateful that our paths have crossed, and I hope to remain in contact with you, long after our graduation. Thanks for all of your help in lab, for making me laugh whenever I was feeling stressed, or just having intense debates about absolutely nothing of merit while we worked. I cannot imagine my time at GSU without you guys. Thank you so much for being there when it mattered.

My family deserves my appreciation more than what I can put into words. I gave my family three weeks' notice that I was moving to Georgia. Although they were shocked, (not to mention, worried) they were nothing but supportive, and they have remained so, through every transition I have made from Tech, to GSU, to my next adventure at UGA. You have all been there, annoyingly positive, even when I was sure I was doomed to fail. You were always there to tell me that I was smart, capable and that I could do anything that I wanted to in life. Between all of you, you have made and raised three successful scientists. I'm not sure how you've managed such a feat, but I'm pretty sure that if you write a how-to book, it would sell like crazy.

Finally, to those friends who have become family: Jorge, Stephanie, and Rebecca. Thank you for being my go-to people when I was stressed, anxious, happy, excited, doubtful—anything. I enjoy venting my frustrations and receiving the most non-sensical, dumb, and, frankly, hilarious advice, in return (though I know in my heart, that you would hop on a plane at the drop of a hat if I asked for it). May we continue to grow old, but never grow up, together. I love you, idiots.

TABLE OF CONTENTS

LIST OF FIGURES

LIST OF ABBREVIATIONS

FA	Fatty Acid
LD	lipid droplet
ATP	Adenine Triphosphate
NADPH	nicotinamide adenine dinucleotide phosphate
PC	phosphatidyl choline
PI	phosphatidyl inositol
PE	phosphatidyl ethanolamine
ER	endoplasmic reticulum
TGs	triglycerides
HSL	hormone-sensitive lipase
Acetyl CoA	acetyl coenzyme A
PKA	protein kinase A
PhosE	phosphoethanolamine
PC3-luc	prostatic carcinoma cell line 3 luciferase
ORO	Oil Red-O
FOV	field of view
NIH	National Institutes of Health
FBS	fetal bovine serum
Ca^{2+}	calcium ion
$[Ca^{2+}]$	calcium ion concentration
$[Ca^{2+}]_i$	intracellular calcium concentration
SERCA	smooth endoplasmic reticulum calcium pump

IP_3	(1,4,5)-inositol triphosphate
GCRs	G-protein-coupled receptors
RTK	receptor tyrosine kinase
$\Delta\mu H$	mitochondrial hydrogen exchange
MCU	mitochondrial calcium uniporter
$[Ca^{2+}]_{SS}$	steady-state calcium concentration
Fura-2-am	fura-2-acetoxymethyl
AM	acetoxymethyl
TMRE	tetramethylrhodamine ethyl ester
$\Delta\Psi$	mitochondrial membrane potential
ROI	region of interest
$[Ca^{2+}]_e$	extracellular calcium concentration
TCA cycle	tricarboxylic acid cycle
HMG-CoA	3-hydroxy-3-methylglutaryl-CoA
FASN	fatty acid synthetase
$FADH_2$	flavin adenine dinucleotide
ATL	adipose triglyceride lipase
MAGL	monoacylglycerol lipase
EDTA	ethylenediaminetetraacetic acid
Thap	Thapsigargin
cAMP	cyclic adenylate monophosphate
UV-Vis	Ultraviolet-Visible
IR	Infrared

FT-IR	Fourier-Transform Infrared
ATR	Attenuated Total Reflectance
COO^-	carboxyl
Asp	Aspartate
Glu	Glutamate
v_{as}	asymmetric vibration
v_s	symmetric vibration
δ	scissoring vibrational mode
CO_2	carbon dioxide
CH_3	methyl
CH_2	methylene
C=O	carbonyl
Abs	Absorbance

1 INTRODUCTION

1.1 Background

1.1.1 Cancer and society

Cancer is the second leading cause of death in the United States and is one of the most prevalent diseases in the developed world[1], [2], [3]. It is the name given to a group of diseases in which the body's cells begin to divide without any checks or balances to stop their proliferation and spread into surrounding tissues[1]. It can arise almost anywhere in the body and be composed of any type of cell. Because of their accelerated growth rate, it can quickly outnumber and force out the "normal" cells within the tissue, forming a tumor.

Under normal conditions, cells undergo a natural death process. When the cell has found itself inviable due to abnormalities in shape, function or DNA damage, released signals force the defective unit to proceed into a programmed cell death[4]. These programmed cell deaths can include apoptosis or autophagy[5]. Necrosis, a third type of cell death, only arises as a result of infection or injury[4]. Cancerous cells, however, find alternative pathways to circumvent programmed cell death, allowing them to continue replicating, unhindered[6]. This leaves researchers searching for ways in which to induce appropriate death progressions to halt tumor growth and cancerous invasion.

Effective treatment for these diseases can vary greatly throughout tissue type and cell subtype due to the vast array of surface markers and alternate pathways for cancer cell survival[6]. Additionally, current cancer treatments aim to inhibit cell proliferation, incurring in negative side-effects, such as the death and slow cell growth of healthy, normal cells[6]. This type of treatment leads to the debilitated, sick state often associated with cancer patients undergoing aggressive chemotherapy[7]. Therefore, the field of cancer research has been interested in finding targeted

approaches, aimed at attacking molecules within the cancer cells that might trigger pathways of natural cell death.

1.1.2 Unique molecular patterns of cancer cells

As mentioned earlier, cancer cells employ the use of several alternative living pathways in order to ensure their survival. These alterations become the biochemical foundation of the cell's tumor-building capacity, aggressiveness and potential for metastasis [8]. Some of the alternative metabolisms favored by cancer cells are aerobic glycolysis, glutamine dependent anaplerosis, which allow cells to migrate from the primary tumor and become viable metastases, and *de novo* lipid generation[8].

Lipid metabolism has been well characterized within cancer cells[9], [10]. The major component of cell membranes are phospholipids, along with other integral lipids, such as sterols and sphingolipids. Due to the constantly replicating nature of cancer cells, they require a steady supply of both structural and energy-providing lipids[10]. This need is what has prompted cancer cells to develop the ability to undergo *de novo* lipogenesis, an ability possessed by only liver, adipose, and lactating breast tissue once the organism enters adulthood[11]. The cells activate lipid anabolic metabolism and attached signaling for subsequent generation of new membranes, storage of energy and as a primary energy source (via fatty acid oxidation) during energy-deficient periods[8].

The cycling of fatty acids (FA) for structural and energetic purposes lies at the center of the lipid metabolism network[10]. These FA can generate metabolic intermediates used in anabolic processes for membrane building blocks or as signaling molecules to activate oncogenic cascades[8] [10]. The balance of FA synthesis and FA oxidation is imperative for the survival of cancer cells. FA are created and stored in reservoirs, known as lipid droplets (LDs), which remain

inactive until needed by the cell. Following the degradation of these LDs, the components created during FA oxidation can aid in the synthesis of membranes, ATP and NADPH required for other processes, and can be used as building blocks for another round of FA synthesis[12] [13] [14] [15]. Because of its important role in cancer cell survival the targeting of lipid metabolism by anticancer medication could very well be the next target for chemotherapies.

1.1.3 Lipid droplets

The demand for FA storage vessels in cancer cells defines a major morphological trademark in cell pathology. In order to have these base materials handy, the cells have employed the use of a special compartment called lipid droplets (LDs), a naturally-occurring organelles that can be found among most eukaryotic cell types[15]. They consist of a phospholipid monolayer studded with integral proteins such as perilipins, that surround a core of triglycerides and sterols. The perilipins allow for the droplets to be enzymatically degraded, so that its contents can be quickly processed for whatever purposes they are needed[15].

It is known that, with the exception of adipocytes, cancer cells possess a higher abundance of these reservoirs, generally of significantly greater size, than normal cell types[10] [16]. While adipocytes use these LDs as more or less static storage units, cancer cells have developed a dynamic life cycle for these vesicles[14]. Due to these differences in metabolic fates, LDs in adipose cells are large and few in number, taking up most of the volume of the cell, while the same organelles in cancer cells are both smaller and more abundant[12] [14]. Their smaller size increases their surface to volume ratio, increasing the rate at which they can be degraded and formed[14].

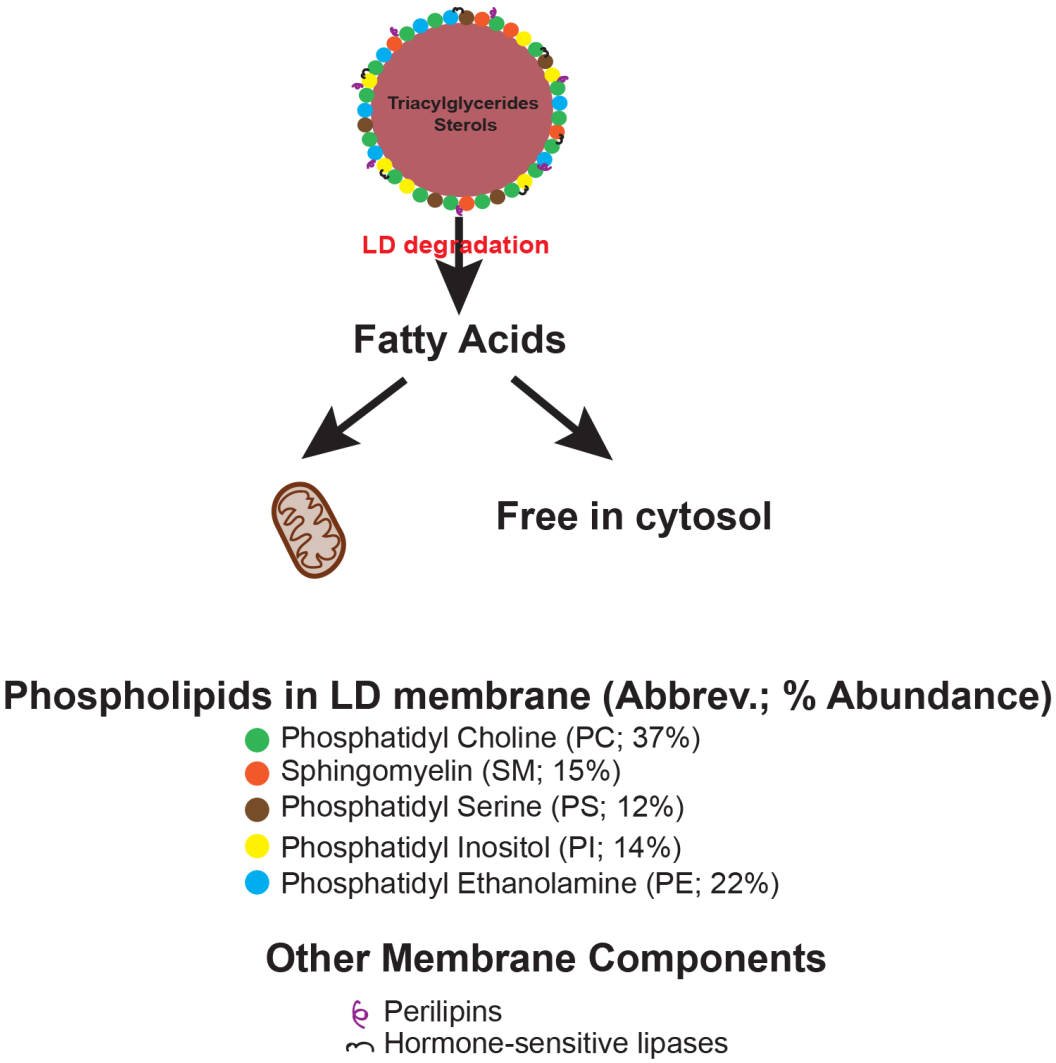

Figure 1.1.1 Schematic representation of lipid droplet structure and its fates

Although there is no definitive mechanism for the creation of LDs, the most compelling model states that LDs are created in the endoplasmic reticulum (ER), through a mechanism named membrane budding [12] [13] [14] [15]. Neutral fatty acids, such as triglycerides and sterols are synthesized in the ER where the components form a film against the membrane[12] [14]. The phospholipid membrane forms a leaflet that then invaginates the neutral lipids of the core before dissociating from the rest of the ER[12]. This results in the creation of a monolayered vacuole with a core of neutral lipids that adopts a naturally round shape. Alternative theories posit that LDs are

extricated from both leaflets of the ER, giving rise to a bicelle[12]. Some scientists favor this theory due to the abundance of surface proteins that seemingly are related to several ER processes[14].

Regardless of how the LDs arise, their presence allows cancer cells to have all the materials they need for rapid proliferation readily available, cutting down on division time and expended energy[15]. In order to unpack the components within LDs, intracellular lipases must hydrolyze the core lipids. These lipids can then be oxidized by the mitochondria to create ATP[14] [15]. Alternatively, they can be shipped elsewhere in the cell for other purposes. In the case of triglycerides (TGs), their release is governed by hormones and activation of protein kinase A (PKA)[15]. PKA phosphorylates the proteins perilipin and hormone-sensitive lipase (HSL), present on the LD surface[12] [15] [14]. This activates a catabolic cascade that ends in the hydrolysis of TGs into fatty acids and glycerol that must be released from the cytosol to avoid cell toxicity[14] [12, 17].

Considering the range of functions which LDs serve in cancer cells, it would help to consider these reservoirs as ideal targets for anticancer treatments. By focusing action on metabolically active LDs, normal cells with little to no lipid droplets, and those with LDs with more static metabolisms would be largely unscathed[18].

1.1.4 Monoethanolamine and its anticancer effects

In cells, the balance of FAs, phospholipids and other lipids is kept through the interconnection of lipid biosynthesis and the Kennedy pathways[18]. Within these pathways, materials broken down into acetyl-CoA from glycolysis or oxidation are reduced to FAs. These molecules are then either converted to FA-CoA and transported to the mitochondria for oxidation or made into phospholipids and exported to the membrane. Disruption of this balance, either by blocking signaling cascades or the sequestration and introduction of materials, would have major implications in cell function and survival.

Previously, our lab has characterized the anticancer effect of monoethanolamine (Etn) on different cancer cell lines. Etn is a small, polar molecule, that serves as a precursor within the Kennedy phospholipid biosynthesis pathway[19]. Once this molecule is phosphorylated to form phosphoethanolamine (PhosE), it can continue down the pathway to create phosphatidylethanolamine (PE), the second most abundant phospholipid present in cells[20] [19] [21]. Due to its ties to these pathways, it is possible that the drug's efficacy *in* vitro is due to a dysregulation within the lipid metabolism[22]. Therefore, the purpose of this study was to evaluate the effect of Etn treatment on a prostate cancer cell line (PC3-luc) signaling mechanisms and its plausible effects on lipid metabolism.

1.2 Overall Objectives

The purpose of this thesis work is to identify the physical and molecular changes relating to the accumulation, storage and metabolism of lipids within prostate cancer cells as a direct result of Etn treatment. To achieve this objective, work will be split up into four aims:

- Aim 1: Histological evaluation of changes in lipid content
- Aim 2: Signaling changes in PC3 cells
- Aim 3: Identification of key players in lipid metabolism-related cell death
- Aim 4: Molecular changes in PC3 cells

1.3 Hypothesis

The effectiveness of Etn as an anticancer substance has been proven in previous work. This drug triggers apoptotic death through the activation of pathways and causes shifts in the abundance of molecules, namely phospholipids, which are intimately related to the lipid pathways. Therefore,

we believe that a portion of Etn's killing potential lies in its ability to disrupt lipid metabolism in a manner that induces cell death.

2 AIM 1: MORPHOLOGICAL EVALUATION OF CHANGES IN LIPID CONTENT

2.1 Introduction

Morphological evaluation of cells has, historically, been a tool used to determine cell structure and function. Because structure and function are closely related, the study of tissues under the microscope, whether stained or unstained, has been a historically used practice to describe and compare cell types or differences between cells[23]. Before the development of biochemical techniques, histology was used to determine the malignancy of abnormal-looking tissues. The idea behind this evaluation is that, because normal structure of tissue had been characterized, any anomaly can be readily identified and attributed to disease. Today, with the use of affinity-based stains, markers, and biochemical assays, we can extract more information from cell and tissue samples than ever before. However, the observation of general morphology of the cells in question still serves as a primary technique to test for differences between two samples.

Individual cancer lines have been developed and immortalized from tumor sources and evaluated both geno- and phenotypically[24]. As such, every cancer type has a certain morphology it follows depending on what tissue it originates from, its capabilities for metastasis, its dependence on adhesion for survival, and whether or not it lives in clusters or single cell populations. The importance of this information is not only to help identify cancerous cells apart from “normal” tissue, but to assess whether or not an intended treatment is having any effect on the essential processes of the cell, changing its characteristics to make it unsuitable for further replication, and eventually dying. This type of characterization has been done for the model cell used in this paper, a prostate cancer cell line derived from a bone metastasis, PC3.

The prostatic carcinoma cell line (PC3) was established in 1979 by Kaighn, et al. They reported of an epithelial cell line that originally derived from the human prostate and could invade

bone to form metastases that they thought would be "useful in investigating the biochemical changes in advanced prostatic cancer cells and in assessing their response to chemotherapeutic agents.[25]" This cell line, while anchorage independent, was well suited for growing in monolayers, agar, 3D soft matrices and suspension. PC3 cells flourish above normal prostate cells in their reduced need for serum and their independence of androgen-specific hormones and growth factors[25]. They are generally spindle-shaped and will anchor flat to the tissue culture surface when grown in monolayer and tend to form close-clustering colonies. These cells also bear physical resemblance to other neoplastic cells with features such as abnormal nuclei, abnormal mitochondria, annulate lamellae and lipoidal bodies[25].

This last feature, the presence of lipoidal bodies, more commonly known as lipid droplets (LDs), has been the basis for research in several fields, including obesity, diabetes, neuroscience, and cancer[12] [15]. They are cytoplasmic organelles that consist of a phospholipid monolayer studded with integral proteins such as perilipins, that surround a core of triglycerides and sterols[15] [14]. It has been shown that these fatty acids extracted through LD hydrolysis has been shown to be incorporated more efficiently into critical pathways compared to those taken up by the cell from the extracellular environment[15]. LDs allow cancer cells to have all the materials they need for rapid proliferation readily available, cutting down on division time, expended energy and making energy sources available for the cell's use. The importance of this structure in the survival of cancer cells make it an ideal target for therapeutics.

In monolayer tissue culture, LDs can be visualized through the use of staining techniques and high magnification imaging. Oil Red-O (ORO) is a diazol dye that stains neutral lipid and cholesteryl esters in bright red but does not stain biological membranes. This diazol dye has little affinity for the solvent that it is in, a mixture of miscible alcohol and water, but has high affinity

for lipids, especially those found within LDs[26]. This effectively incorporates the dye into the cell and tags all of the reservoirs. The addition of a counterstain, such as hematoxylin for nuclear and cytoplasmic differentiation allows to distinguish LDs within the cell, as opposed to LDs released by lysed cells that have not been removed from the slide with the washing steps.

Following fixing and staining of the monolayer cultures, cells can be visualized on a brightfield microscope with a high magnification, such as 100 x. Because the dye can be visualized within the visible light spectrum, there is no need for lasers or specialized lamps in order to quantitate the results. Additionally, through the image acquisition of several fields of view (FOV) per sample, the relative density of LDs per FOV can be calculated. This is achieved through the use of the National Institute of Health's (NIH) software, ImageJ[27]. Essentially, the amount of red within an image, or "positive ORO staining area" is measured relative to the amount of blue counterstain, or "total area occupied by a cell", under a set of permanent parameters[28]. This staining and image quantification technique is a low-cost, robust, quantitative manner to identify average amount of lipid staining in cancer cells whether they be grown under normal conditions or with the addition of a therapeutic.

Treatment of prostate cancer cells with exogenous Etn has been shown to induce apoptosis in prostate cancer cells[19]. Within the cell Etn is one of many molecules involved in the phospholipid biosynthesis pathway. Its metabolism yields the creation of lipids, fatty acids, phospholipids, and sterols that are the building blocks of new cells[11]. There is no definitive answer as to how Etn affects the cell in order to induce apoptosis. Therefore, it was of interest to see whether Etn treatment affected lipid reservoirs in the cells. The combination of ORO staining and image analysis with ImageJ would allow for the visualization of any possible changes within the cytoplasmic content of LDs between Etn treated and control cultures.

2.2 Aim 1 Objectives

- Validate cancer cell model by identifying LDs in cancer cell line PC3-luc
- Visualize morphological changes between treated and untreated cells (shape, size, LD number, etc)
- Use software to digitally quantify relative amount of lipids in each sample

2.3 Hypothesis

Due to its anticancer properties, the use of exogenous Etn should have a visible physical impact on the morphology of the PC3 cell line. Previous studies in the Aneja lab have shown that treatment with Etn causes the reduction of certain phospholipids within the cell, including phosphatidyl choline, sphingomyelin, phosphatidyl serine and phosphatidyl ethanolamine. All these are present within the monolayer of the LDs[19]. Therefore, Etn's use on cancer cells should affect LDs by either distorting their surface to volume ratio or the disruption of their protective phospholipid monolayer.

2.4 Materials and Methods

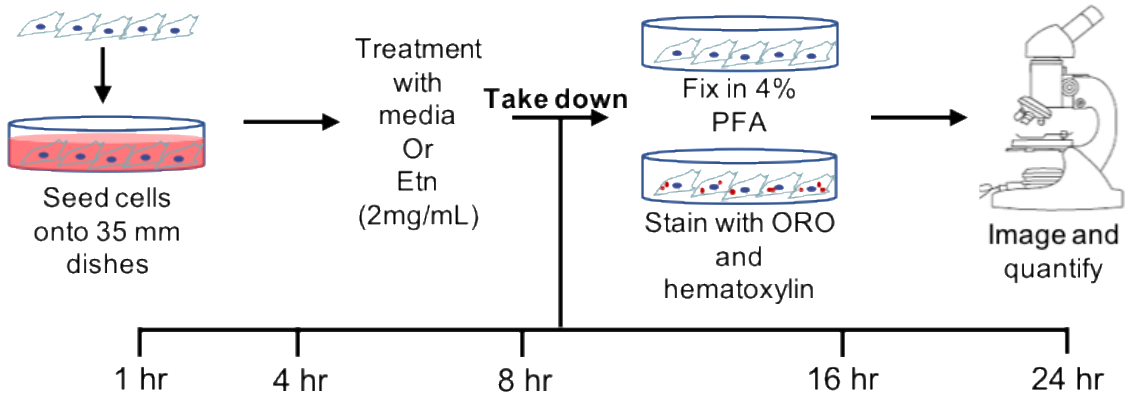

Figure 2.4.1 Schematic overview of methodology used in Aim 1

2.4.1 Cell culture

PC-3-luc cells (Perkin Elmer) were cultured in complete media containing 10% fetal bovine serum (FBS, GE Health) and 1% penicillin-streptomycin (Pen-Strep, Corning), under normal culturing conditions (37 °C, 5% CO_2).

2.4.2 Oil Red-O staining

Oil Red-O staining (Sigma, cat #O-0625) was done on control and 2mg/mL Etn-treated PC-3-luc cells cultured in 35 mm Petri dishes. Plates were then incubated under normal conditions, and taken down in matched pairs at 1, 4, 8, 16, and 24 hrs. At each timepoint, cells were fixed in place with 4% paraformaldehyde for fifteen minutes and washed with phosphate buffered saline (PBS). Samples were washed with 60% isopropyl alcohol and stained with Oil Red-O dye (5 mM, 5 mins) before washing under tap water until solution ran clear. Dishes were counterstained with Harris' hematoxylin solution (Sigma, cat # HHS16, 1 min) and washed as before. Coverslips were mounted with glycerol and dishes were kept in the refrigerator until imaging.

2.4.3 Oil Red-O imaging and analysis

Fixed, stained dishes were imaged on a Zeiss Axio A-100 microscope with a 100x magnification, oil-immersion objective. 10-15 images (Axio 2 Imager 2 LED camera) were taken per timepoint, per group for densitometry analysis. Images were color thresholded on ImageJ software, to select all red pigmentation, and measured relative to the amount of space occupied by cells in each FOV. Percent of staining was calculated as follows:

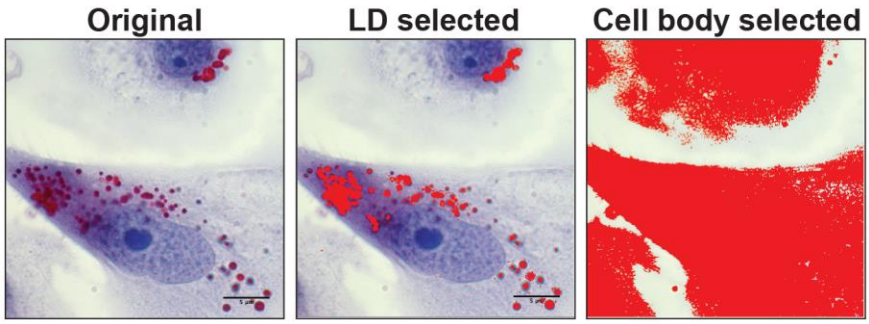

Figure 2.4.2 Selection of LDs and cell body for ImageJ analysis

Percent of staining was calculated as follows:

$$\%\text{Oil Red-O staining} = \frac{\text{Positive ORO staining area}}{\text{Total occupied area}} \; X\ 100$$

Measurements of each group, per timepoint were compared via ANOVA with Tukey's. P-values were determined with unpaired t-tests.

2.5 Results

PC3 cells have been characterized and in use for the purpose of drug research since their development in 1979. As their other cancerous relatives, they contain LDs that allow them to thrive in their environment by providing energy and structural components for rapid proliferation. These LDs could be targeted as part of an anticancer therapeutic. Given Etn's proven effectiveness against several cancer cell lines, including PC3, the purpose of this study was to observe its effect, if any, on the LD population within the cell and quantify that effect using digital analysis techniques.

In cell samples treated with Etn, there were a few notable morphological changes when compared to the control. These cells are epithelial-like in shape, and so, they extend out their cytoplasm to increase their available surface area for nutrient exchange. Within the first three time

points (1, 4 and 8 hrs) there appears to be cell rounding in the treated group (Figure 2.5.1 F-H) when compared to the control group at the same time points (Figure 2.5.1 A-C). This cell rounding comes accompanied with the loss of definition of the borders of the cell's cytoplasm, suggesting a weakening, loss of elasticity or adverse effects to cell adhesion properties of the cytoplasmic membrane in the presence of Etn. Additionally, vacuole-like structures are present in the cytoplasm of treated cells that are not present in the control group (black arrow heads). In general, there is a visible reduction of LD content in treated cells as compared to their respective controls.

Densitometry analysis of ORO staining required the relative amounts of red in the image, known as "positive ORO staining area" be ratiometrically compared to the total area of the FOV that was occupied, or "total occupied area", as previously described in the methods. ORO staining comparison between control and treated groups resulted in the significant decrease of positive red staining in treated groups (Figure 2.5.1 K) for the first four time points. This reduction correlates with the visual decrease of LDs seen in panels A-J.

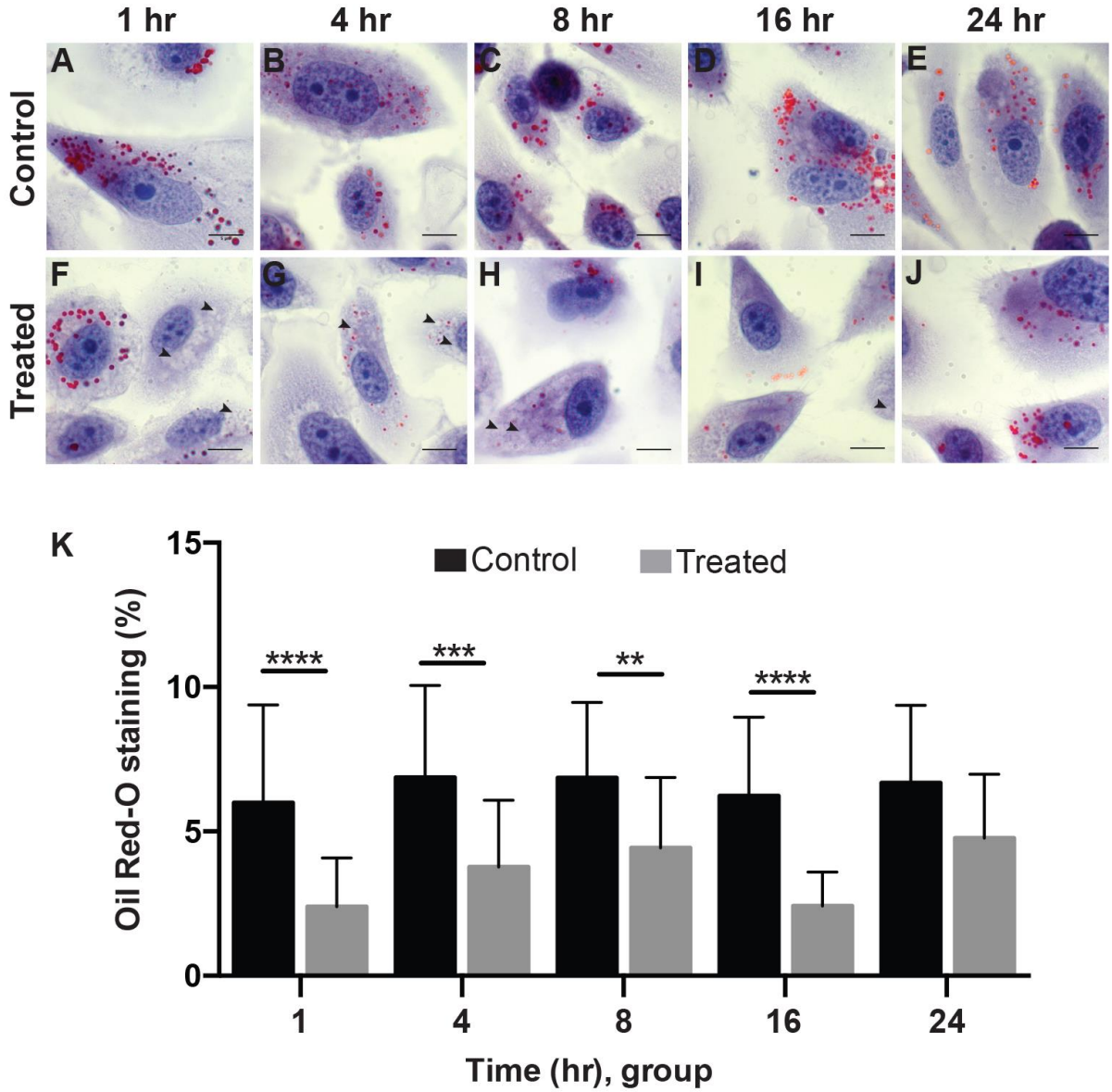

*Figure 2.5.1 Oil Red-O Quantification of stained PC3 cells at various timepoints. Representative images of monolayer culture of PC3 cells under control (A-E) and treated (F-J) at all time points. Quantification of positive Oil Red-O staining (K) uncovered significant differences in lipid droplet content. Treated cells (gray bars) show a significant decrease in positive Oil Red-O staining at several time points when compared against control (black). Results seen as mean ± standard deviation. Scale bars = 5 μm. Significant differences defined as * = p value < 0.05, ** = p value <0.01, *** =p value < 0.005, ****=p value < 0.0001.*

2.6 Discussion

LDs are a cell organelle found in most eukaryotic cells and are part of the cell's dynamic lipid metabolism. In cancer cell lines, these LDs provide the energy and materials necessary for the cell to quickly divide and flourish in low-nutrient environment. The framework of this experiment sought to uncover whether the Etn's mode of action involved, in part, the disruption of the cell's lipid metabolism. Through the use of basic lab techniques such as cell culture, cell staining and microscopy, it was possible to visually compare the amount of positive lipid staining in PC3 cells under either normal growth medium conditions or Etn treatment.

Gross visual analysis of the cell's morphology revealed a change in cell shape of Etn treated groups at early time points in the form of filopodia retraction and cytoplasmic disruption. This caused the cells at earlier time points to appear rounded and vacuole-like structures in the cytoplasm in Etn-treated samples, characteristics not present in the control group. Additionally, the confines of the cell, as established by the cell membrane, did not exhibit the opaque or feathered edges seen in the treated group. Poorly defined borders might be a sign of cell membrane weakness brought on by treatment. Moreover, the number of LDs visible within the cell cytoplasm seemed to be reduced in the experimental group. This reduction might help explain the loss of cell membrane definition, as there are less sterols and lipids on hand to create the membrane, the cells make do with whatever materials present. Cell shape and LD number seemed to normalize by 24 hrs.

Images acquired for each of the samples were further analyzed through the software ImageJ. About 10-15 images per group, per time point were evaluated under the same hue, saturation and brightness thresholds in order to subjectively analyze LD density within cells. Quantitative analysis of ORO staining was concurrent with the gross analysis of images. Within the first four

time points (1, 4, 8 and 16 hrs.), there was significant decrease in LD density in the cytoplasm of Etn-treated cells than their control group counterparts. Much like the cell shape recovery, LD density also normalized within 24 hours of treatment. This can be due to the combination of the degradation of Etn in the media along with the fact that these cells undergo a division approximately every 23 hrs. Any Etn-resistant cells, which would have been unaffected by treatment, would have divided into a new generation on the plate, reestablishing the LD levels in the cytoplasm per FOV.

2.7 Conclusion

Etn is a small molecule with proven anticancer properties. While its mechanism of action is not entirely known, previous publications have linked its therapeutic use in cancer cells in the activation of several pathways that lead to cell death. The purpose of this study was to determine whether Etn activates pathways that disrupt the lipid metabolism by affecting change to the cell's lipid reservoirs. Through staining, microscopy and digital analysis of acquired images, it was determined that Etn does, indeed, affect LD content in cell cytoplasm when compared to control population, at several time points. Although cell population recovers LD content at 24 hrs, Etn's targeted impact on the LD population at early stages of treatment make it a strong candidate as a non-toxic, daily, oral anti-cancer regimen in order to maximize its effects. Additionally, Etn treatment brings about a change in general cell morphology. In conclusion, Etn causes a disruption in lipid metabolism that can be appreciated through low-cost computational methods. With these results in mind, the next step was to identify what signaling pathways related to apoptotic death were affected by this metabolism disruption.

3 AIM 2: SIGNALING CHANGES IN PC3 CELLS

3.1 Introduction

Calcium, in its ionic form Ca^{2+}, is the most common signal transduction molecule in cells of all types[29] [30]. Ca^{2+} is essential for cell growth and survival, and due to the extent of its effects upon the cellular network, it is difficult to assign its effects to one universal mechanism. Intranuclear Ca^{2+} increases initiate gene expression and cell cycle progression, but also can activate degradative processes in programmed cell death[31]. This is due to the fact that prolonged high calcium concentration ($[Ca^{2+}]$) activates nucleases that cleave DNA and degrade cell chromatin[31]. Therefore, the concentrations of Ca^{2+} inside and outside the cell have to be tightly regulated, lest they trigger the cell's own demise.

Though required for normal cell functions, calcium cannot be metabolized in the same way other second-messengers are recycled[29]. Under normal physiological conditions, the concentration of intracellular calcium ($[Ca^{2+}]_i$) is approximately 100nM, which is about 20,000-fold lower than the average $[Ca^{2+}]$ in the extracellular environment[29]. Increased $[Ca^{2+}]$ within the cell can cause toxicity and will eventually lead to cell death, which means that the cell has to develop mechanisms to chelate and store Ca^{2+} in an inert state to maintain stable $[Ca^{2+}]_i$[29]. For this purpose, the cell employs two types of Ca^{2+} buffers, both mobile and immobile, that will trap and bind the ions in a secure formation until needed.

From a molecular standpoint, Ca^{2+} ions are able to coordinate a large amount of oxygen atoms in their primary array spheres (4-12 atoms)[29] [32], though common coordination spheres arrange 6-8 oxygen atoms per calcium ion[32]. Specific calcium-binding proteins use this coordination to tightly sequester the ion through glutamate and aspartate residues that are charged at biologically relevant pH[29]. This sequestration acts as a Ca^{2+} buffer that increases in binding

capacity as intracellular calcium concentration increases[30]. The action of these buffers affect the rate of diffusion of calcium ions throughout the cell, making it one of the slowest diffusing ions[32]. These proteins can be suspended in solution, acting as a mobile buffer, and in smaller cells, they are sufficient to control $[Ca^{2+}]$[29].

In eukaryotic mammalian cells, however, increased cell size means that the use of mobile buffers alone is not sufficient to regulate the concentration of Ca^{2+} within the cytoplasm[29]. In this case, the use of immobile buffers, in the form organelles with the capability to trap and store the ions within their confines, are employed[31]. The biggest intracellular Ca^{2+} store is the endoplasmic reticulum (ER). The ER is a large three-dimensional network of membranes that is employed in packing away materials into vacuoles. The ER acts as an anchor to Ca^{2+}-binding proteins, and actively sequesters Ca^{2+} into the intraorganellar space[30]. Specialized ATP-dependent pumps, known as the smooth ER calcium (SERCA) pumps move Ca^{2+} from the cytoplasm into the ER where proteins, such as calsequestrin, bind the calcium in a dynamic storage, to be released only under certain signals have been received to deliver Ca^{2+} to the cytosol[29].

There are different mechanisms to slightly increase $[Ca^{2+}]$ in the cytosol. Ions from the extracellular environment and the ER are transported into the cytosol across the plasma membrane or from the ER through ion channels, respectively[29]. In non-excitable cells, such as cancer cells, the inositol (1,4,5)-triphosphate (IP_3) pathway predominates in calcium signaling[33] [34]. Both G protein-coupled receptors (GCRs) and receptor tyrosine kinases (RTKs) release IP_3[29] [33]. GCRs activate phospholipase Cβ, while RTKs stimulate phospholipase Cγ to convert phosphatidylinositol (4,5)-bisphosphate into IP_3 and diacylglycerol[29] [31] [33] [34]. IP_3 acts as an intracellular second messenger that triggers the release of Ca^{2+} from the ER by binding to its receptor in the ER[33]. This Ca^{2+} release can increase $[Ca^{2+}]_i$ from 100 nM to almost 1μM[29]. For

Ca^{2+} to enter cells by crossing the plasma membrane, the membrane must be depolarized[35]. Open potassium channels force the membrane potential to more negative potentials, drawing Ca^{2+} more rapidly across the plasma membrane[29] [36]. Ca^{2+} then enters through voltage-independent Ca^{2+}-specific ion channels[29].

The ER is not the only organelle that acts as an immobile buffer for Ca^{2+}. Mitochondria accumulate Ca^{2+} at up to 0.5mM levels in the mitochondrial matrix owing to a large electrochemical gradient by mitochondrial hydrogen exchange ($\Delta\mu H$)[31] [37]. Avoiding mitochondrial Ca^{2+} overload is energetically demanding for the cell, which has evolved a number of transport mechanisms to control energy expenditure[31]. Ca^{2+} concentrations in the mitochondrial matrix are controlled by a balance of influx and efflux pathways. Mitochondrial Ca^{2+} uniporters (MCU) control the influx of the ion. They have lower affinities for Ca^{2+} than SERCA pumps and are only significant when cytosolic Ca^{2+} rises above ~0.5μM, activated by external Ca^{2+} and the allosteric effect of adenine nucleotides[31] [38]. Efflux is controlled by Na^{+}-H^{+} or Ca^{2+}-Na^{+} exchangers. Some studies suggest that the mitochondria's sensitivity to the release of Ca^{2+} from the ER means that there are close contacts between both organelles that are involved in molecular crosstalk[31].

Reactions within the mitochondrial matrix lead to the synthesis of several molecules, including nucleotide precursors and fatty acids that give rise to phospholipids[31]. In tandem, the mitochondria play a role in the homeostasis of Ca^{2+} within the cell, giving rise to effectors that can link calcium fluctuation to changes in energy metabolism[39]. Substantial evidence has built up in recent years indicating that metabolic regulation is only one of the roles of the mitochondrial Ca^{2+} signal[31]. In particular, the role of mitochondrial Ca^{2+} reserves in the intrinsic cellular signaling for triggering cell death is well established[39] [40].

In order to induce apoptosis, early cell death events must induce the release of cytochrome c from the mitochondria and Ca^{2+} from the ER into the cytosol[29] [31] [40]. The release of cytochrome c from a small subset of mitochondria will activate the IP_3 pathway, therefore releasing Ca^{2+} from the ER into the cytoplasm[30]. This will create a feedback loop that will drive the release of cytochrome c from the majority of the cell's mitochondria, forming the apoptosome and leading to caspase activation, eventually triggering cell death[29] [31] [40]. The mitochondrial pathway of apoptosis is regulated by members of the Bcl-2 protein family, including: Bcl-2, and Bax and Bak, acting as anti- and pro-apoptotic proteins, respectively[31]. In cells that circumvent programmed cell death, like cancer cells, Bcl-2 has been shown to act in Ca^{2+}-storing organelle membranes, such as ER and mitochondria to reduce the steady-state $[Ca^{2+}]$ ($[Ca^{2+}]_{SS}$) in the ER to diminish the effect of the apoptotic signal[31] [36].

In order to avoid accidentally triggering cell death, $[Ca^{2+}]_{SS}$ must be maintained through a delicate balance of calcium influx to the cytosol and efflux to the extracellular space or ER[29]. Certain conditions involve cells foregoing the process of programmed cell death once the unit reaches senescence, prompting scientists to find tools to trigger apoptosis and get rid of the abnormal cell[31]. Among these tools live-cell imaging has become a widely recognized resource to track fluctuations in Ca^{2+} release and changes in mitochondrial polarization. The use of fluorescent tags, sensitive to these two factors are able to give qualitative and quantitative comparisons of control and treated cells to determine treatment effectiveness.

Fura-2-acetoxymethyl ester (Fura-2AM) is a membrane-permeant ratiometric dye that measures $[Ca^{2+}]$ by fluorescence[41]. Once the dye is incorporated into the cell cytosol, cytosolic and organelle esterases convert the acetoxymethyl ester (AM) forms into Ca^{2+}-sensitive carboxylic forms[41]. This Ca^{2+}-induced fluorescence has maximum emission at 340 and 380 nm[41]. Excitation

at these wavelengths results in differences in emission intensities, the ratio of which is used to determine the $[Ca^{2+}]_i$[41]. The use of a fluorescent ratio allows for the normalization of variables of cell thickness or dye concentration that may lead to false results, making it a robust measurement for intracellular Ca^{2+}.

Tetramethylrhodamine ethyl ester (TMRE) is a rhodamine-derived fluorescent dye known as a "redistribution dye"[42] [37]. This dye is able to cross the plasma membrane into the cytosol where its lipophilic character, charge and solubility allows it to accumulate within the inner mitochondrial membrane space[42]. The distribution of the free dye across the inner membrane of the mitochondria follows the Nernst equation, where its uptake is dependent upon electrical potential across the membrane ($\Delta\Psi$)[42] [37]. The flux of Ca^{2+} across the mitochondrial membrane can cause changes in $\Delta\Psi$ due to the ion's poor electronegative exchange potential compared to traditionally used H^+[29]. TMRE can be used as a qualitative assessment of tandem signaling pathways affection both normal Ca^{2+} signaling and mitochondrial function as a response to an external stimulus.

The use of exogenous Etn has been shown to cause cell death in different cancer cell lines, including PC3. Etn-treated cells expressed higher levels of pro-apoptotic markers and a decrease of anti-apoptotic markers that are classically Ca^{2+}-sensitive[19]. Therefore, it was of interest to evaluate if Etn's effectiveness was in any way related to the activation of Ca^{2+} apoptosis pathways in the ER and mitochondria. In order to test this, the use of live cell imaging using Ca^{2+}- and $\Delta\Psi$-sensitive dyes (Fura-2AM and TMRE, respectively) was employed with healthy PC3 cells to track Ca^{2+} and $\Delta\Psi$ fluctuations before and after Etn treatment. In the case of fura-2AM imaging, the measurements were taken in both Ca^{2+}-rich and -depleted conditions. Measurements were taken in both conditions as a manner to pinpoint the source of Ca^{2+} leaks into the cytosol. If the

environment in which the cells are contained lacks Ca^{2+} sources, it would stand to reason that Ca^{2+} entering the cytosol comes from intracellular stores, such as the ER or mitochondria.

3.2 Objectives

- Track changes in Ca^{2+} signaling of healthy cells following Etn
- Ca^{2+} influx versus Ca^{2+} release from internal stores
- Determine the effect of Etn on mitochondrial membrane potential

3.3 Hypothesis

Ca^{2+} is the most common signal transducer in the cell, impacting the function and integrity of all organelles, including the ER, nucleus and mitochondria. Previous studies in the Aneja lab have reported the positive effect of Etn in the increase and decrease of pro-apoptotic and anti-apoptotic markers, respectively. Among the affected markers Bax and Bcl-2, Ca^{2+}-sensitive mitochondrial proteins, were present. Therefore, we hypothesized that Etn induces cell death through Ca^{2+}-dependent pathways involving the activation of caspase through the mitochondria.

3.4 Materials and Methods

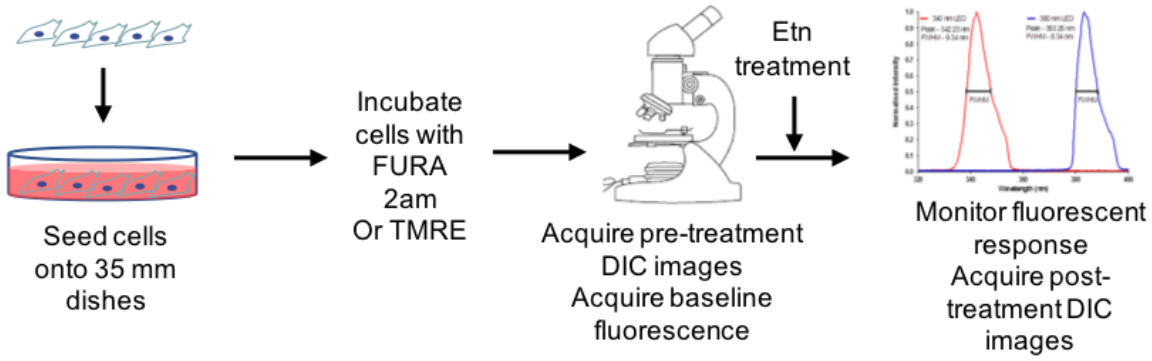

Figure 3.4.1 Schematic representation of methodology used for Aim 2

3.4.1 DIC Imaging

An Olympus microscope equipped with the water-immersive objective (40X), DIC filters, and acquisition and offline analysis software (Till Photonics, FEI, Germany) were used for acquiring DIC time-lapse images of PC3 cells and their lipid droplets.

3.4.2 Live cell ratiometric intracellular Ca^{2+} imaging.

An Olympus microscope equipped with the water-immersive objective (40X), ratiometric dichroic mirror with 340/380 split, 400 nm long-pass emission filter and acquisition and offline analysis software (Till Photonics, FEI, Germany) were used for acquiring ratiometric time-lapse images of fura 2 fluorescence in the cytoplasm of PC3 cells.

Cells were loaded with 5 μM fura-2 AM (Molecular Probes, Eugene, OR, USA) for 30 min at 37C, washed 3 times with the extracellular solution (see pharmacological agents) and incubated for another 20 min at 37C. Acquisition and analysis of calcium images were conducted using Live Acquisition and Offline Analysis software (Till Photonics, FEI, Germany). Time-lapse images were acquired every 30 min after 100 ms exposure at 340 nm and 380 nm excitation light and 420

nm long-path emission filter. The ratio of emission fluorescence intensities at 340nm excitation to 380nm excitation was used to assess changes in intracellular calcium concentration. PC3 cells were excluded from analysis if their pretreatment ratios of $[Ca^{2+}]_i$, exceeded 0.7, which indicated a calcium concentration above normal resting cytosolic values of calcium, as established in earlier experiments [43].

3.4.3 Live cell mitochondrial potential imaging

Cells were incubated with tetramethylrhodamine, ethyl ester (TMRE) (Molecular Probes, Eugene, OR, USA), the mitochondrial potential dye for 30 mins at 37C, and subsequently washed three times. Cells were observed on an Olympus fluorescent microscope, equipped for live imaging using a 40x magnification, water immersion objective and Live Acquisition software. Images were acquired using 535 nm excitation and a long path 590 nm emission filter. Time-lapse images were acquired every 30 seconds. The intensity of fluorescence was measure in the region of interest (ROI) that included one or a few mitochondria. Baseline measurements for mitochondrial potential were taken as a control before adding Etn to a final concentration of 2mg/mL. Mitochondrial polarization was then tracked for an additional 20 mins.

3.5 Results

Live cells imaging provides information in real-time of cellular responses to external stimuli, such as drug treatments. In this study, the fluctuations in $[Ca^{2+}]_i$ and $\Delta\Psi$ were evaluated using fura-2am and TMRE fluorescent dyes, respectively. Ca^{2+} was measured in conditions in which external Ca^{2+} was and was not readily available (Figure 3.5.1). While using fura-2AM dye, a fluorescence intensity ratio baseline was taken on healthy cells within the ROI. This baseline

was 0.50 and 0.37 in Ca^{2+}-containing (black line) and non Ca^{2+}-containing media (grey line), respectively. Following baseline reading and normalization, Etn was added dropwise into the observation dish to a concentration of 2mg/mL (red arrow). A solvent control was used to discard the possibility of fluctuations due to addition solution to the observation dish. Increase in fluorescent ratio was observable within the first 30s (first measurement following treatment), reaching its peak at around 2 mins in Ca^{2+}-containing media and 3 mins in non-Ca^{2+}-containing media. Once at its peak, fluorescent ratio normalized to near-baseline levels, indicating that Ca^{2+} increase was a transient event. Fluorescence was monitored for 30 minutes following Etn addition to capture any long-term effects. An extracellular solution-only control did not yield a response (Appendix A).

In the case of $\Delta\Psi$ fluctuation using TMRE dye, a fluorescence baseline of healthy cells within the ROI was similarly acquired (Figure 3.5.2). Etn was added dropwise into the observation dish (red arrow) to a concentration of 2mg/mL. Within 2 mins of treatment there was a 15% increase in fluorescent intensity that is immediately followed by a sustained decrease of signal. This increase and subsequent decrease correspond to a moment of hyper- and depolarization of the mitochondria, respectively. Fluorescence was monitored for approximately 30 minutes following treatment to capture any long-term effects. An extracellular solution-only control did not yield a response (Appendix A).

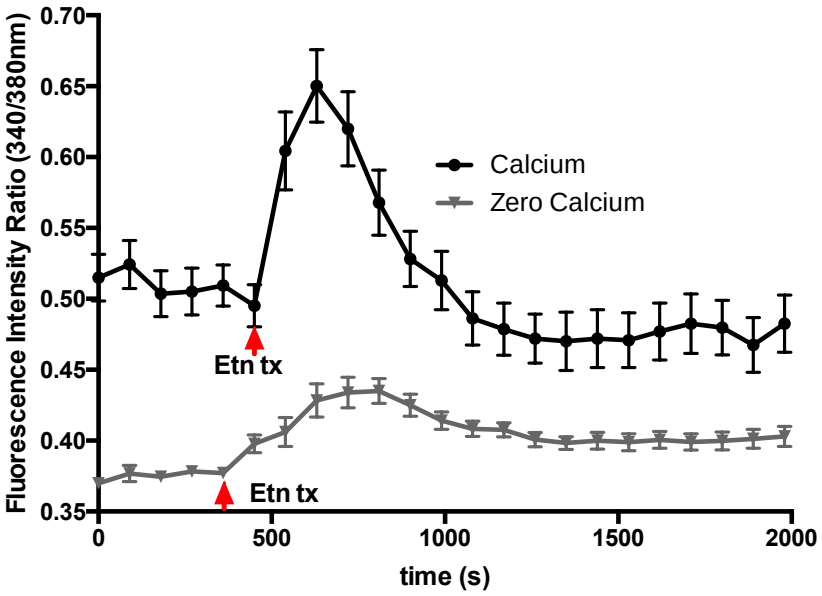

Figure 3.5.1 Calcium-dependent fluorescence in PC3 cells before and after Etn treatment. Black line denotes experiment done in solution containing 2 mM Ca^{2+} present. Gray line denotes experiment done in solution with no added Ca^{2+} and EDTA present as a Ca^{2+} chelator. In both cases, transient increases in calcium signaling followed the addition of Etn. Results shown as mean ± SEM Graphs are average of n=5 ROI, N=3.

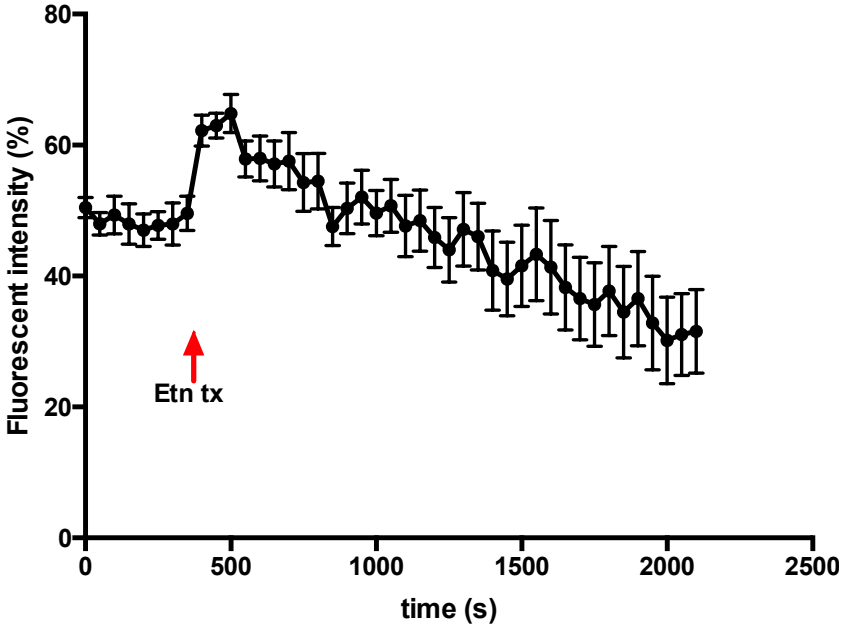

Figure 3.5.2 Mitochondrial potential of PC3 cells before and after Etn treatment. Moment of hyperpolarization, followed by sustained depolarization resulted from the addition of Etn to observation plate. Results shown as mean ± SEM. Graphs are average of n=5 ROI, N=3.

3.6 Discussion

The traffic of calcium ions through multiple calcium channels are responsible for a plethora of cellular responses necessary for normal cell function. Previous data collected in the lab led to the question of whether Ca^{2+} mediated pathways were responsible to the induction of cell death of PC3 cells following treatment with Etn. Fura-2AM, was used to measure $[Ca^{2+}]_i$, Its ratiometric property allows imaging software to calculate an accurate fluorescence by comparing the intensity of emission at 340 and 380 nm in order to accurately calculate $[Ca^{2+}]_i$. Measurements were recorded in conditions where extracellular calcium was and was not available ($[Ca^{2+}]_{ex} = 0$),. In both cases, a transient increase in calcium signaling can be observed approximately 2 minutes following Etn treatment (Figure 3.2).

The rates of transient Ca^{2+} increase differ depending on whether or not there are external sources of Ca^{2+}. The sharp rise of the intensity of fluorescence in Ca^{2+}-rich conditions compared to slower rise in Ca^{2+}-free conditions is indicative of Ca^{2+} influx from the extracellular environment in order to replenish the Ca^{2+} stores within the cell or the depolarization of the plasma membrane, opening the voltage-gated Ca^{2+} channels and allowing ions to the cytosol. This transient increase in $[Ca^{2+}]_i$, that was independent on the presence of extracellular calcium suggests Etn-induced calcium release from intracellular stores. This increase in $[Ca^{2+}]_i$, in turn, can affect the polarization of the mitochondrial membrane, leading to the activation of $[Ca^{2+}]_i$,-mediated cell death pathways through the release of cytochrome c [31] [30].

Following transient Ca^{2+} increase in both conditions, baseline fluorescence did not return to control levels. This difference may be attributed to the availability of Ca^{2+} in the environment and the tight regulation of Ca^{2+} homeostasis in the cytosol. In conditions where Ca^{2+} is available in the extracellular matrix, the cell must work to sequester ions released from organellar stores to

maintain normal $[Ca^{2+}]_i$ (100nM). The opposite is true for cells that were observed in $[Ca^{2+}]_e$=0. A Ca^{2+} chelator is added to the solution to guarantee a near zero and insignificant concentration of Ca^{2+} in the extracellular environment, leaving Ca^{2+} leaked out of the plasma membrane to become unavailable for re-entry. This may cause the cell to prevent further sequestering into the ER or mitochondria until a point in time where exchange between intracellular and extracellular Ca^{2+} sources, as it occurs normally, can be re-established. Perhaps a longer observation of cells in both conditions see the fluorescence returning to control baseline levels.

Having established a change in $[Ca^{2+}]_i$ following Etn treatment, it was of importance to review the impact of this change on the cell's mitochondria. The compounding of changes in mitochondrial potential and $[Ca^{2+}]_i$ could point towards the triggering of Ca^{2+}-mediated cell death pathways as the source of Etn's effectiveness. A fluorescent polarization marker, tetramethylrhodamine, ethyl ester (TMRE), was employed alongside live cells imaging to track changes in $\Delta\Psi$. The addition of Etn led to a brief hyperpolarization period, followed by a sustained depolarization of the mitochondria (Figure 3.5.2) around the same time in which changes in $[Ca^{2+}]_i$ occur. It may be possible that the Ca^{2+} release from the mitochondria initiates the release of Ca^{2+} from ER, causing the initial hyperpolarization before going into sustained depolarization.

Previously, our lab has shown that treatment of PC3 cells with Etn led to a decrease of Bax and an increase in Bcl-2 expression, all necessary for the initiation of apoptosis. In order to substantiate these assumptions, further experiments on the effect of intracellular Ca^{2+} stores in the process of apoptosis are required. The idea behind this would be to determine whether the emptying of intracellular Ca^{2+} stores, such as the ER and mitochondria prior to Etn treatment will delay apoptosis. If so, then the conjunction of these results points towards Ca^{2+}-aided initiation of

apoptosis signaling cascade due to the activation of Bax, the decrease of Bcl-2 and the release of cytochrome c from the mitochondria.

3.7 Conclusion

The effects of Ca^{2+} changes within the cell activate a diverse range of pathways necessary for normal cell growth, function and the initiation of programmed cell death. The effects of calcium signaling are widespread and can involve different organelles, including the ER and the mitochondria. Transient increases in $[Ca^{2+}]_i$ can induce the formation of the apoptosome by the activation of apoptotic markers and the release of cytochrome c from the mitochondria due to changes in mitochondrial membrane potential. Etn causes the transient increase of Ca^{2+} in the cytosol of healthy cells through the depletion of intracellular calcium stores and import of Ca^{2+} from the extracellular environment. This depletion of intracellular stores accompanies a simultaneous dysregulation of $\Delta\Psi$. Taking these results into consideration with previous data of Etn decreasing the activity of anti-apoptotic markers and increasing the activity of pro-apoptotic markers we can conclude that part of Etn's effectiveness comes from the activation of Ca^{2+}-dependent apoptotic pathways. This increase in intracellular Ca^{2+} may also be the trigger of Ca^{2+}-dependent hormone stimulated lipolysis. Measurement of the rate of lipolysis with and without the emptying of ER Ca^{2+} stores prior to treating with Etn would conclusively link the transient Ca^{2+} increase with the changes in LD content seen in Aim 1.

4 AIM 3: IDENTIFICATION OF KEY PLAYERS IN LIPID METABOLISM-RELATED CELL DEATH

4.1 Introduction

Lipids are an essential macromolecule for healthy cell function[10] [9]. They comprise of a group of hydrophobic molecules that include triacylglycerides (TAGs), sterols, sphingolipids, and phospholipids and are necessary at a cellular level for energy storage and structural purposes[9]. Fatty acids (FA) are the building blocks for TAGs, part of lipids that are stored within LD stores, whereas phospholipids, sterols and sphingolipids are the major components of all biological membranes[9] [44]. In addition to energy and structure, lipids can have roles in cell signaling, some working as second messengers and hormones for the purpose of communication between cells[9]. It has been established that lipid metabolism within cancer cells greatly differs from the metabolism of "normal" healthy tissue[10] [9] [44] [45] [46]. These changes can affect cell growth rate, proliferation, differentiation and motility[45].

Most eukaryotic mammalian cells import their lipids from the extracellular environment, rather than making their own[10] [9]. FA and lipoproteins are synthesized in the liver or adipocytes from the breakdown of carbohydrates. These molecules enter circulation and are taken up by cells to use as energy or to store them in the form of LDs[9] [44]. Fetal and undifferentiated cells possess the ability to create their own lipids in a process known as *de novo* lipogenesis[10]. However, once cells differentiate into mature cells, only a handful of cell types, including liver, adipose and lactating breast tissue, retain this ability[10].

In order to make FA, cells use acetyl groups provided by citrate from the tricarboxylic acid cycle (TCA) and convert it into acetyl-coenzyme A (acetyl-CoA) and oxaloacetate in an adenine triphosphate (ATP)-dependent reaction[9] [10] [45]. Oxaloacetate is then converted into pyruvate and

nicotinamide adenine dinucleotide phosphate (NADPH), which is used in the pentose phosphate pathway to make lipids[10] [9]. Acetyl-CoA is transformed to malonyl-CoA in an enzyme-catalyzed reaction, subsequently acetyl and malonyl groups are coupled to the fatty-acid synthetase enzyme[10] [9]. The condensation of acetyl groups generates a 16-carbon saturated FA known as palmitic acid[10] [9]. This FA is elongated and desaturated in the cytoplasmic face of the ER membrane[10] [9]. Desaturation alters the newly-synthesized FA's physical properties in order to create species suitable for either plasma membrane creation (sphingolipids, phospholipids) or energy storage (triacylglycerides)[10] [9].

Another important process within lipid metabolism is the mevalonate pathway, from which cholesterol is synthesized[9] [45]. This process involves the condensation of acetyl-CoA with acetoacetyl-CoA to form 3-hydroxy-3-methylglutaryl-CoA (HMG-CoA)[9] [45]. The reduction of HMG-CoA to mevalonate by HMG-CoA reductase represents the rate-limiting reaction of this pathway and is highly regulated[9] [45]. Cholesterol is an important component of cell membranes, responsible for modulating the fluidity of the bilayer and forming detergent-resistant microdomains called lipid rafts that can also be used as signal transducers[9] [45] [44]. Additionally, sterols form the backbone of hormones, and so, are important in their synthesis. Previous studies have identified the accumulation of cholesterol as a hallmark of prostate cancer[45].

Cancer cells are characterized by proliferation rates that are faster than their healthy counterparts[10] [9] [45] [46]. This high proliferation rate requires large amounts of lipids in order to create new membranes[10] [9] [45] [46]. Scientists discovered long ago that cancerous tissues possess the ability to undergo *de novo* lipogenesis in a manner similar to embryonic tissue[10]. Some cancers, like breast and prostate, are characterized by an increased expression of fatty acid synthetase (FASN), which suggests that fatty acid synthesis is an important part of pathogenesis[10]

[9] [44]. However, the source of these FAs may determine the phospholipid composition of the membranes due to the cell's limited ability to synthesize polyunsaturated FAs *de novo*, as they do not possess the enzyme Δ 12 desaturase[44]. This means that cancer cell membranes are enriched with a mixture of saturated and monounsaturated FAs, which are less prone to lipid peroxidation, and, therefore, more resistant to oxidative stress-induced cell death[9] [44]. Saturated lipids are more densely packed, which alters membrane dynamics that limit uptake of materials from the extracellular environment, such as drugs, which poses a problem with targeted therapies[9] [44].

Most cancer cells exhibit an increased consumption of glucose, which they break down through the glycolytic pathway to create lactate, regardless of the availability of oxygen, a phenomenon known as the 'Warburg Effect'[44] [10]. It is possible, however, to break down FAs for energy through a process called β-oxidation[44] [9]. In this process, cytoplasmic free-FAs are coupled to CoA and transferred to carnitine by the enzyme carnitine acyltransferase and shipped into the mitochondrial matrix[44] [9]. After entering the mitochondria, the acyl chains are recoupled to CoA, where it undergoes several steps of oxidation and hydration, yielding NADH and flavin adenine dinucleotide ($FADH_2$), as well as acetyl-CoA that can enter the tricarboxylic acid (TCA) cycle[44] [9]. In the case of prostate cancer, tumors exhibit low rates of glucose consumption, increased FA uptake, and an increased dependence on β-oxidation of FAs as their main source of energy[44] [9]. Additionally, prostate cancers have been shown to overexpress certain markers, such as elongases leading to the production of very long FA chains that may play a role in cancer transformation[44] [9] [10].

Different cancer cell types have different preferences as to where they mainly source their FA[44]. Although, it is generally acknowledged that *de novo* lipogenesis is an active pathway, it is possible to use exogenous FAs to substitute endogenously made FAs[44]. Therefore, the majority

of cancer cell types maintain a balance of both lipogenic and lipolytic pathways to fill their FA needs, depending on their environment, in order to ensure survival. [44] For example, aggressive breast cancers that lack normal markers, known as triple-negative breast cancer, express a lipoprotein lipase, which is capable of breaking down extracellular lipids and use transmembrane mechanisms to incorporate the free-FAs created[44] [9] [10]. Regardless of where the FAs originate, however, excess materials (both FA and sterols) are stored within LDs in the cell cytoplasm[9] [44]. Stored FAs can be unpacked and transported for energy generation through a series of lipases, among them, hormone-sensitive lipase (HSL), adipose triglyceride lipase (ATL), and monoacylglycerol lipase (MAGL)[44] [9] [10].

Intracellular lipolysis catalyzes the breakdown of FA necessary for proliferation, growth and cancer cell migration[44] [9] [10]. This lipolysis is promoted by lipases that de-esterify contents of LDs and create free-FA and glycerol in a process called lipophagy and is used by cells to adapt to stress and prolong cell survival[9] [44]. In addition to providing resources and energy for the cell, lipolysis helps cells avoid toxicity through the accumulation of saturated FAs (such as palmitate) and subsequent triggering of apoptosis[9] [44]. This accumulation of saturated FAs serves as a feedback loop to inhibit further FA synthesis until the cells are in need of material to transform into energy[9] [44]. Thus, it is necessary for the processes of lipogenesis and lipolysis to be balanced within the cell in order to maintain lipid homeostasis[44]. However, it is not known whether FAs obtained endogenously versus those acquired exogenously enter metabolic pathways for membrane and energy in equal measures, or whether one is preferred over the other for different applications.

Calcium is known to be the effector of several different pathways within the cell, including those related to lipid metabolism[29] [30]. In studies involving adipocytes, it has been shown that

hormone-sensitive lipase activity was directly proportional to the amount of Ca^{2+} present in the system and that its effects could be ebbed through the introduction of a Ca^{2+} chelator, such as EDTA[47] [48] [49]. High $[Ca^{2+}]_i$ activate cyclic adenylate monophosphate (cAMP) levels, either directly (through Ca^{2+} and/or calmodulin, CaM) or indirectly (through CaM kinase or protein kinase C) [50]. This increase in [cAMP], in turn, activates protein kinase A (PKA)[49] [50]. PKA is an enzyme used to phosphorylate other proteins within the cell[50]. In the case of LDs, PKA hyperphosphorylates perilipins, a family of proteins found on the surface of LDs and are meant to protect the LD from the action of lipases[49] [50]. Once phosphorylated, the perilipin changes conformation on the LD surface, allowing lipases, such as HSL, to degrade the neutral lipids within the LD[49] [50]. Although these mechanisms have been studied in adipocytes and hepatocytes it is likely that cancer cells follow a similar pathway due to their similarities in lipid metabolism.

The ubiquity of Ca^{2+} makes it difficult to tease out the effects it has on observed pathways[29]. Although there are few tools for studying Ca^{2+} pumps, thapsigargin, a sesquiterpene lactone, irreversibly inhibits SERCA pump in a specific manner by trapping it in its Ca^{2+}-free state[51] [52]. This means, that once the ER stores are emptied, and the $[Ca^{2+}]_c$ is high, there is no way for the cell to pump the ion into the ER for sequestering[51] [52]. Thapsigargin provides a platform for comparison between Ca^{2+} store- and non-Ca^{2+}store- stimulated cellular responses.

In the previous aim it was established that the reduction of $[Ca^{2+}]$ within Ca^{2+} stores has protective effects toward a variety of inducers of cell death, such as ceramide and oxidative stress. Moreover, the introduction of this aim has talked about the differences in lipid metabolism between normal and cancerous cells, including the delicate balance between lipogenesis and lipolysis. Due to the results seen in previous experiments, it was of interest to determine whether the Etn-stimulated disappearance of LDs within the model PC3 cells was due to increased lipolysis or the

inhibition of LD creation. In order to study this question, a colorimetric biochemical assay was used.

During lipolysis TAGs are degraded into free-FAs and glycerol molecules that are exported from the cell cytoplasm into the extracellular environment[44] [9]. In order for the glycerol to be recycled, it must be phosphorylated in the liver to form glycerol-3-phosphate[10]. Due to the constraints of cell culture, once expelled from the cell, glycerol remains in solution within the media. The free glycerol assay uses an enzyme complex to phosphorylate and oxidize the glycerol from collected media which creates peroxide that reacts with the colorimetric probe. The saturation of the color probe (and, in so, the absorbance of the sample) is directly proportional to the amount of glycerol within the sample, yielding a robust, quantitative result that can be calculated in concentration against a standard curve.

4.2 Objectives

- Probe whether LD reduction comes as an effect of Etn-induced lipolysis
- Evaluate whether there is a connection between the reduction in LD content seen in Aim 1 with the transient increase in Ca^{2+} seen in Aim 2.

4.3 Hypothesis

Enhanced or abnormal lipid metabolism is one of the hallmarks of cancer cells. Because these cells rely heavily on lipids and their metabolites to create energy and make the materials to aid in rapid proliferation, the destruction of LDs where these lipids are stored could prove to be an important therapeutic target. Data collected in the previous aims support the possibility of cells undergoing increased lipolysis due to Etn-treatment, as we see a decrease in LD presence in the cytoplasm, meaning a reduction of stored lipids, and a transient increase in Ca^{2+}, which can induce many lipolytic pathways within the cell.

4.4 Materials and Methods

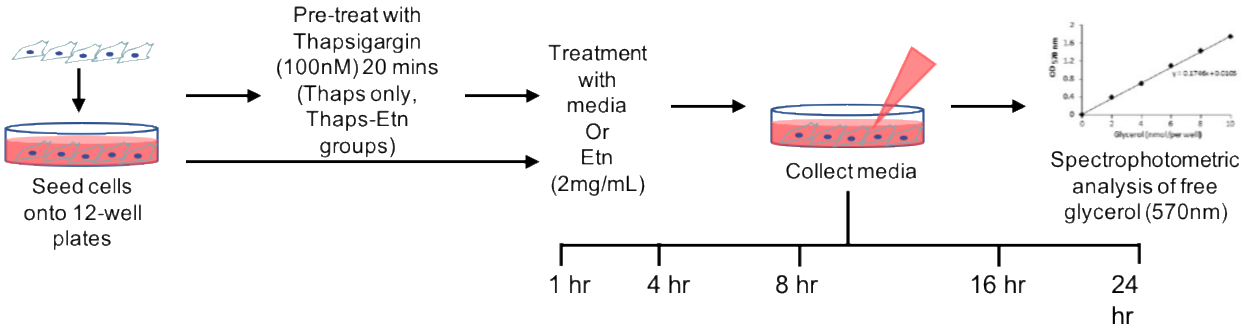

Figure 4.4.1 Schematic representation of methodology used in Aim 3.

4.4.1 Lipolysis assay

PC-3-luc cells were seeded at a density of 350,000 cells/mL onto 12-well plates, overnight. Control and 2mg/mL Etn-treated plates were incubated for 1, 4, 8, 16, and 24 hrs, wherein media was collected from the plates. Additional plates were seeded in a similar fashion and treated with 100 nM Thapsigargin for 20 mins before being exposed to Etn for 1 hr. Positive controls (media only, Thapsigargin only) and negative controls (Etn only) were run alongside experimental group and collected in same manner.

Collected media was analyzed using the Free Glycerol Assay kit (Sigma), as per manufacturer's instructions. Briefly, 10uL aliquots of the samples were pipetted into a 96-well plate and allowed to incubate at room temperature in the dark with active enzyme buffer and indicator for 10 minutes following moderate shaking. Plate was read on a UV-Vis Spectrophotometer (Molecular Devices) at 570 nm. Results were analyzed against a standard curve to determine glycerol concentration per sample. Results recorded as mean ± standard deviation and analyzed using ANOVA with Tukey's.

4.5 Results

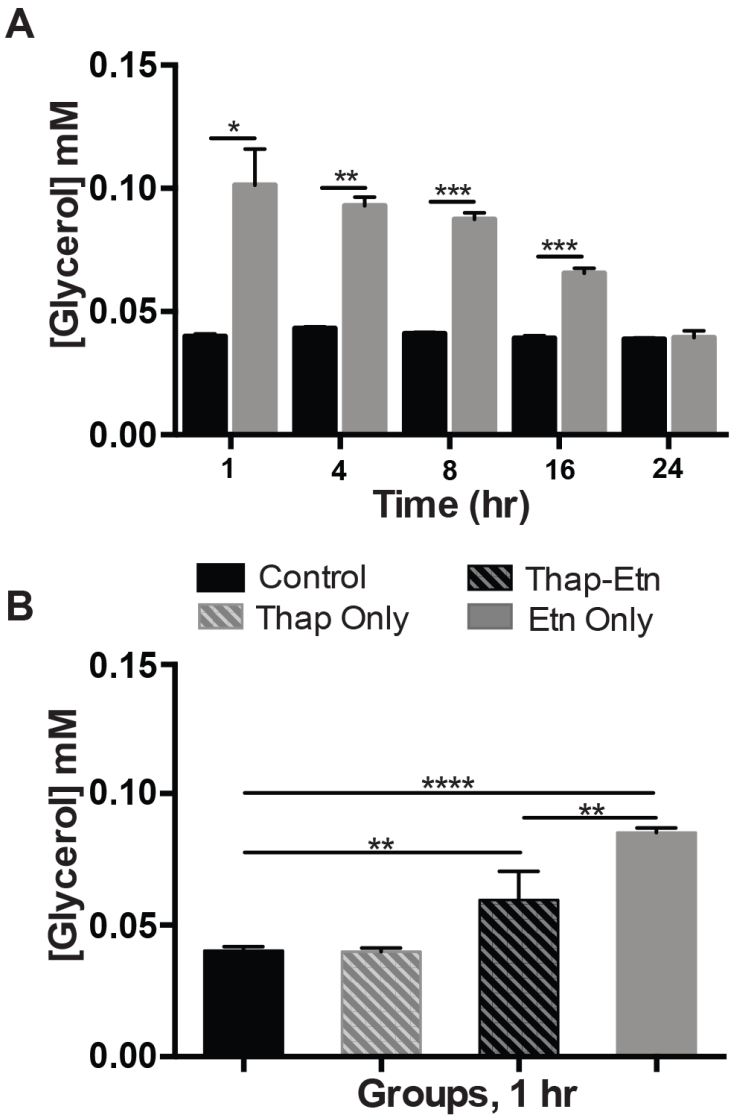

Figure 4.4.1 Quantification of free glycerol in control (black) and treated (gray) cells as a measure of lipolysis.

In a timed experiment, Etn treatment significantly increases the amount of glycerol released into the extracellular medium as early as 1 hr following treatment, normalizing by 24 hrs (A). These findings are consistent with ORO staining results seen in Figure 1. Cell samples pre-treated with thapsigargin, a SERCA pump inhibitor, release a lower amount of glycerol into extracellular environment following Etn treatment. Thapsigargin only control behaves similarly to media control (B). Results in mean ± standard deviation. p>0.05=; p>0.01= **; p>0.005=***; p>0.001=****.*

Abnormal lipid metabolism is a critical part of cancer cell survival, proliferation and invasion, and any disruption in the processes involved could cause catastrophic effects. Therefore, we endeavored to evaluate whether there was any difference in lipolysis occurring within the cells following Etn treatment, and if there was any change in lipolysis rate through time. The amount of free glycerol in media was measured in control and Etn-treated cell culture wells as an indicator of lipolysis at five different time points (1, 4, 8, 16 and 24 hr). Spectrophotometric analysis of collected media presented with increased concentrations of free glycerol at 1, 4, 8, and 16 hours, normalizing to near-control levels by 24 hours (Figure 4.2A). Amount of glycerol in the media of the control group remained in an average of 0.040 ±0.002 mM throughout all time points. Cells treated with Etn released an average concentration of 0.101 ±0.015 at peak lipolysis 1 hr following treatment and steadily decreased to 0.039 ±0.003mM, 24 hrs after.

Seeing as there was a more than two-fold increase in free glycerol within the media in Etn-treated samples as compared to control samples, it was imperative to investigate whether this lipolysis was driven by a Ca^{2+}-dependent mechanism. Two groups were pre-treated with the SERCA pump inhibitor, thapsigargin, before either being treated with Etn or used as a control, in addition to the original control and treated groups. Cells underwent Etn treatment for 1 hr, as this is foreseeably the longest the cell can withstand without incurring in significant stress due to lack of Ca^{2+}. At 1 hr of treatment, there was no difference between media and thapsigargin control samples. Although both thapsigargin-Etn and Etn-treated cells had a significant increase in glycerol compared to control (0.060 ±0.011, 0.085 ±0.002, 0.040 ±0.002 mM, respectively), cells that were pre-treated with thapsigargin contained approximately 30% less glycerol in the media in comparison to its Etn-only counterpart (Figure 4.2B), suggesting that Ca release from intracellular stores (or a functional ER) is necessary for part of the effect of Etn on lipolysis.

4.6 Discussion

Cancer cells thrive under a delicate balance of lipogenesis and lipolysis that allows them to grow, proliferate and invade healthy tissue at an accelerated rate[44]. They are able to utilize lipids as energy sources, building materials and signaling molecules to direct their growth in order to thrive in the microenvironment they are to inhabit[46]. These responses depend on the activation of different pathways that will evaluate their need to store or utilize synthesized or imported lipids at any given time. The relationship between calcium and lipolysis has been thoroughly studied in the context of adipose tissue. Intracellular calcium can modulate the rate at which lipids are broken down by the cell through the stimulation of several pathways, including the HSL pathway[47] [48].

The introduction of exogenous Etn to healthy PC3 cells has already been shown to have an effect on lipid stores in Aim 1. The marked decrease of positive LD staining was visible as soon as 1 hr following treatment and was not normalized to near-control levels until 24 hrs following initial treatment. Therefore, it was of importance to determine whether this significant decrease was due to the blocking of new LD formation following normal metabolism of lipids or, as hypothesized, the accelerated dismantling of LD structures in a process of increased lipolysis. Evaluation of free glycerol in the media of control and Etn-treated samples confirmed the increase of lipolysis within treated groups at 1, 4, 8, and 16 hrs following treatment, normalizing at 24 hrs (Figure 4.2 A). Knowing that increased lipolysis was occurring within treated cells, it was critical to determine whether this lipolysis was induced, whether totally or in part, through Ca^{2+}-dependent pathways.

Ca^{2+}-dependent lipolysis, such as the hormone stimulated pathway (HSL), has been reported in lipid-rich cells, like adipocytes, as one of the major roadways to lipid homeostasis[50]. Due to the ubiquitous nature of Ca^{2+} in the cell it is difficult to claim that lipolysis seen in Figure

4.2 is due solely to the transient increase in Ca^{2+} seen in Aim 2. Utilizing a known Ca^{2+} pump inhibitor, thapsigargin, the rate of lipolysis was measured in thapsigargin-pre-treated groups against normal control and Etn-treated samples. The idea behind this experimental design was to deplete the cell's internal Ca^{2+} stores and observe whether there was any difference to the lipolytic response once cells were treated with Etn. However, it was of utmost importance to maintain the time course of the experiment short, as to not stress the cell due to lack of intracellular Ca^{2+} reserves and the implications that a low Ca^{2+} availability could have on essential processes. Interestingly, while the cells pre-treated with thapsigargin before Etn exhibited increased lipolytic activity as compared to control samples, there was a marked decrease in lipolysis when compared to the Etn-only group. Media-only and thapsigargin-only controls had similar rates of lipolysis (Figure 4.2 B). This data suggests that Ca^{2+} is paramount for the activation of lipolysis.

Though it is possible that Ca^{2+} is not the only second messenger that is participating or responsible for this response, this data supports the proposed role of $Ca^{2+}{}_i$ in the activation Etn-induced lipolysis. The HSL pathway, as described before, involves cation exchange from Ca^{2+}-binding proteins and the phosphorylation and several enzymes prior to the eventual esterification and degradation of LDs. This signaling cascade means the alteration of molecular charges and protein structure of many, if not all, the players involved[49] [50]. Therefore, it is possible that these changes can be observed through a high-resolution, vibration-based technique, such as Raman, photoacoustic or Infrared spectroscopy. The analysis of control and treated samples through these methods may yield information about protein sidechain coordination, such as electronegativity fluctuations between bonds, that will correlate to the known steps of the HSL pathways.

4.7 Conclusion

In order to ensure that cancer cells have the resources necessary for rapid growth and proliferation there must be a balance between the processes of lipogenesis and lipolysis. Changes within calcium and mitochondrial signaling can affect downstream processes, such as the activation of lipolytic pathways, led by calcium-sensitive species[12] [14] [15]. Previous aims have demonstrated a reduction in LD content within the cytoplasm (Aim 1) and a transient Ca^{2+} increase (Aim 2) following Etn treatment. Therefore, it was important to look at lipolysis in the context of these two observations. The amount of free glycerol in the media was significantly increased in time points where a marked reduction of LD content was observed in Aim 1 (1, 4, 8, 16 hrs), confirming the claim that LD disappearance was due to Etn-induced lipolysis. Additionally, the introduction of a SERCA pump inhibitor, thapsigargin, as a pre-treatment led to decreased rates of lipolysis when compared to Etn-only groups. Hence, the Etn-induced state of lipolysis within PC3 cells is due, in part, to Ca^{2+}-mediated processes, such as the HSL pathway. The findings within this experiment allow for the exploration of the use of other Ca^{2+}-channel agonists in the treatment of cancer.

5 AIM 4: MOLECULAR CHANGES IN PC3 CELLS

5.1 Introduction

The release of Ca^{2+} from intracellular stores into the cytoplasm is possible only due to the conformational change of proteins sequestering the ions, whether it be through oligomerization, phosphorylation or cationic exchange[29] [53]. Further than a physical alteration, this change in structure, along with the downstream effects of Ca^{2+} release (as is the inducement of lipolysis) has an impact on the overall molecular makeup of the cell[54]. These molecular changes are transient and cyclical in healthy cells, as the increase and decrease of [Ca^{2+}] is tightly regulated in order to maintain homeostasis[29]. However, a sharp increase due to the administration of a drug can be distinguishable from normal metabolic patterns through high-sensitivity techniques.

Infrared spectroscopy (IR) is a one of the classic techniques for the study of small molecular structures[54] [55]. It is an integral part of biological research due to its large application range, high resolution, low acquisition time and small sample size requirement[54] [55]. The IR range of radiation (780 nm to 1mm wavelength) is absorbed by the electrons within a molecule[54] [55]. This radiation causes an excitation of the electrons, which in turn stimulates their vibration and oscillation in specific patterns known as transitions[54] [55]. The vibrational frequency depends on the strength and polarity of the vibrating bonds, making them susceptible to the intra- and inter-molecular changes[54] [55]. The absorption bands will depend on both the type of bond (whether it is single, double or triple), the mass of atoms at either end of the bond, the electromagnetic pull of atoms donating or withdrawing electrons, from either within the molecule or those in the microenvironment[54] [55]. The strength of absorption has a proportional value to the increasing polarity of the molecule, meaning that all polar bonds can contribute to the IR spectra[54].

The IR spectra is represented in a plot as absorption as a function of the inverse of wavelength, or wavenumber (ν), with the unit cm^{-1}[54]. Typically, wavenumbers run from high to low, from left to right, following the plotting convention for wavelength (small to large). The range in which IR radiation exists can be separated into three regions: i) near-IR, 780-2500 nm, ii) mid-IR, 2500-50000 nm, iii) far-IR, 50000 – 10^6 nm. Mid-IR is the area most commonly observed when looking at biological systems, with wavenumbers ranging from 4000-200 cm^{-1}[54] [55]. This is due to the fact that thermal energy at room temperature is approximately 200 cm^{-1}, making mid-IR the first level of vibrational excitation following ground level vibrational excitation[54].

Modern IR spectroscopy is commonly Fourier Transform Infrared Spectroscopy (FT-IR). FT-IR possessed an interferometer with fixed and movable mirrors that generate a variable path between two beams that give the detector a signal[54] [55]. Light emitted by the source is split in two: one that is sent towards the detector and another that is reflected onto the moveable mirror and back towards the detector[54] [55]. When the beams combine destructive and constructive interference will occur, according to the wavelengths absorbed and emitted by the sample[54] [55]. The light intensity is relative to the optical path difference creates an interferogram in the form of a Fourier Transform[54] [55]. Another Fourier Transform done by the computer yields the spectrum that can be interpreted[54] [55]. The main advantage of FT-IR is that it is a method of rapid data collection and high light intensity the detector which responds with a high signal to noise ratio[55].

Samples can be analyzed either in transmission, transflection, or attenuated total reflectance (ATR) [54] [56] [57] [58]. Previously ATR was favored over transmission because it allowed a sample to be placed on a crystal without worrying about pathlength of the beam to the sample[54] [56]. IR light is directed towards the sample at an angle of incidence that is totally reflected at the interface of the sample and the scaffold where it rests[54]. This reflection incites the sample before

the light is reflected towards the detector to create the interferogram[54]. The sample could be mounted onto the slide to form a thin film with easily exchangeable buffer[54] [56] [57] [58]. Modern FT-IR spectrometers, however, are equipped for dry transmission analysis, and have been popularized by biological analysis[59] [60] [61]. Here, the sample (whole cell, protein sample or extract) is reconstituted in a small amount of buffer and placed upon $BaCl_2$ slides and dried under a gentle vacuum in a nitrogen chamber[59] [60] [61]. This allows for whole structures to be analyzed in situ without any major damage to the sample[59] [60] [61].

Though vibrational frequency changes due to changes in structure, it is impossible to determine structure of a molecule from IR spectra[54] [55] [61]. This is due to the fact that all polar bonds (bonds between atoms of different electronegativity) will create a band on the spectra, which can overlap and be difficult to deconvolute[54] [55]. However, it is possible to see changes, if any, in the structure through the migration, change of shape or intensity of specific IR bands[54] [55] [61] [62]. Vibration-based methods are so sensitive that they can detect changes as small as 0.002% in vibration due to the bond distortions arising from changes in bond length and strength[54].

Additionally, vibrations in adjacent bonds of a molecule, like those that contribute to 3D structure, can affect each other[54]. As an example, changes in the amino acid side chains of proteins due to protonation or ion capture provoke the shift and disappearance of bands and is often used to measure enzymatic activity of certain proteins[54] [55] [57] [58] [61] [62]. A characteristic vibration that has been studied is the coupled carboxyl (COO^-) vibrations of amino acid residues that act as cation chelators within the cell, as are the aspartate (Asp), glutamate (Glu) resides in the case of Ca^{2+} sequestration coordination[54] [29]. Some of the most commonly observed vibrational areas are depicted in Figure 5.1. In this figure, common vibrational modes of biologically abundant molecules are depicted (symmetric, asymmetric, scissoring, etc.) Each set of vibrations is also

associated to a macromolecule which are the more likely sources to the specific bands, and so, every vibration depicted is also color coded to correspond.

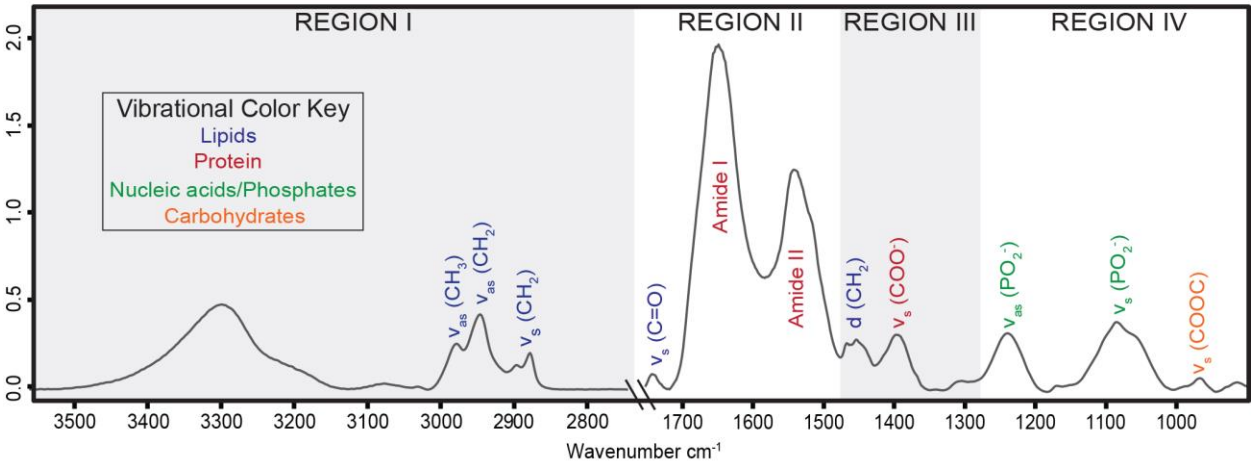

Figure 5.1.1 Commonly observed FT-IR spectral regions in biological samples

As discussed in the previous aims, the treatment of PC3 cells with Etn has yielded results in the form of the decrease of LD content within the cell cytoplasm, the transient alteration of $[Ca^{2+}]_i$, and the inducement of lipolysis through pathways involving Ca^{2+} signaling. These responses are all consequences of molecular alterations taking place within the cell, interrupting normal functions and prompting its death. The hypothesis presented here has been that Etn's effect is intrinsically linked to the changes in lipid metabolism via the disturbance of normal Ca^{2+} signaling. Etn causes a transient increase in Ca^{2+}, promoting the activation of cAMP, and subsequent activation of PKA[50]. PKA will then hyper-phosphorylate perilipins on the surface of LDs, leaving space for HSL to unpack and degrade the LDs[50] [63] [64]. The neutral lipids within the LD are degraded into glycerol and FAs that get exported out of the cell to be recycled by other cells, or used for energy, respectively[50]. All of these alterations have an effect on the vibrational patterns of the cell's molecules.

The loss of LD component stores, cation exchange from Ca^{2+}-binding proteins, phosphorylation and 3D structure change of other proteins such as perilipins all represent possible alterations to molecular vibrations [54] [55]. While it may not be possible to deduce specific changes in lipids or structure between control and treated cells, it would be possible to note if there are any fluctuations in vibration corresponding to common protein or lipid bond conformations[59] [60]. Therefore, we endeavored to launch a pilot study the effects of Etn on PC3 cells at a molecular level. While the results discussed below are preliminary findings, we believe that, with proper standardization, FT-IR could be a valuable technique for screening potential anticancer drugs based on the alteration of specific vibrations relating to the lipid metabolism.

5.2 Objectives

- Evaluate changes within the total molecular composition of prostate cancer cells as a result of Etn using FT-IR spectroscopy

5.3 Hypothesis

Treatment of PC3 cells with Etn results in the dysregulation of Ca^{2+} signaling and the induction of lipolytic pathways, leading to a marked decrease of LD in the cytoplasm. With this information in mind, it is only fitting to assume that there is an overall shift in the vibrational patterns associated with different macromolecule functional groups within the cell. Therefore, wavenumber differences in stretching and vibrational patterns between control and Etn treated PC3 cell samples are expected to be observed.

5.4 Materials and Methods

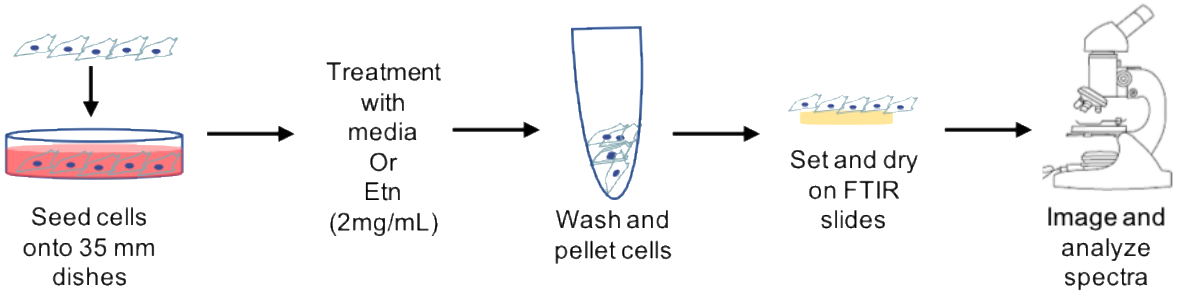

Figure 5.4.1 Schematic representation of methodology used for Aim 4

5.4.1 Fourier Transform-Infrared Spectroscopy (FT-IR)

PC3 cells were cultured on 35 mm dishes in standard conditions (37 °C, 5% CO_2) until 90% confluency. Dishes were treated with media containing 2 mg/mL Etn or regular maintenance media, as a control. Following 4 hours of treatment, cells were pelleted and washed with cold PBS to remove any residue of media or drug. Pellets were resuspended in approximately 20 uL of PBS and dotted onto FT-IR transmission coverslips and dried under a gentle vacuum for 20 minutes. Sample spectra was acquired on a Varian 600 UMA Fourier Transform Infrared Spectrophotometer (FT-IR). A background scan was taken of each slide, and control and experimental samples were measured fifteen times per each sample triplicate (N=32 scans/measurement). Resulting spectra was normalized to the Amide I peak, a rubber band baseline correction was applied, and was analyzed for second derivative.

5.5 Results

Fourier Transform Infrared spectroscopy (FT-IR) is a classic analytical technique that allows for the observation of vibrational patterns of polar bonds within a molecule. The advantage of the technique lies in its ability to detect the vibrations and stretching patterns from the bond between any two atoms with differing electronegativities This yields a wealth of information about how the atoms within a system of interest interact with each other under normal and experimental conditions. Due to the computerized nature of modern FT-IR systems, collected data can be used to instantly create second derivative graphs and focus on specific regions of interest to the researcher. separate spectra into distinct regions allow for ease of reading and concentrated analysis of specific regions. The purpose of this experiment was to determine if the use of Etn as an anticancer drug yielded any observable molecular changes in healthy PC3 cells as compared to control samples, in an effort to develop a low cost, rapid screening system using FT-IR in the future.

Evaluation of control and Etn-treated samples on the high field of the mid-IR spectra (~3100-2800 cm^{-1}), two areas that had significant changes that could be linked to specific vibrations (Figure 5.5.1). Peak shifts at ~2960 and ~2872 cm^{-1} (Red notches on spectra and circles on 2^{nd} derivative) represent changes in the symmetrical and asymmetrical vibration of CH_3 molecules, respectively, commonly associated to lipids. This area of the FT-IR spectra is closely related to the vibration of hydrophobic bonds within molecules that are less likely to shift due to their close interaction to avoid polar substances. Although the high wavenumber region does not offer as much information in biological systems as those with lower wavenumbers, the fact that there is a shift within this area points to the possibility of larger changes in the remainder of the spectra.

Within mid-wavenumber field of the mid-IR (~1700-1300 cm^{-1}) contains vibrations of bonds that are more polar and hydrophilic in nature, lending itself to molecules such as the charged amino acid residues of proteins and parts of the phospholipid backbone. In this area, represented in Figure 5.5.2, there are changes apparent in 4 areas of the spectra, reflecting 5 shifts within the second derivative spectra. Of particular interest is the shift of peak ~1743 cm^{-1}, which represents vibrations of ester bonds within lipids, and the shifts of amide I and II (~1650 and ~1550 cm^{-1}). Amide I and II are composed of the overlap of several protein-related vibrations relating to secondary structures, such as α-helices and β-sheets/β-rolls, in addition to negatively charged amino acids that coordinate sequestration processes and cation exchange. The changes seen in the second derivative graphs may hint to a change in protein structure due to Etn treatment.

The low-wavenumber region of the mid-IR spectra (~1300-900 cm^{-1}) changes relating to nucleic acids and phospholipid backbone bonds are observed. The bands appearing at ~1241 and 1085 cm^{-1} exhibit a difference in proportion (ratio of band A to band B) and change of shape when compared to the control. Finally, this area of the spectra also contains a shift in symmetric carbohydrate vibration (C-O-O-C, ~975 cm^{-1}). Together these changes might point towards the denaturation of genetic material in Etn-treated cells.

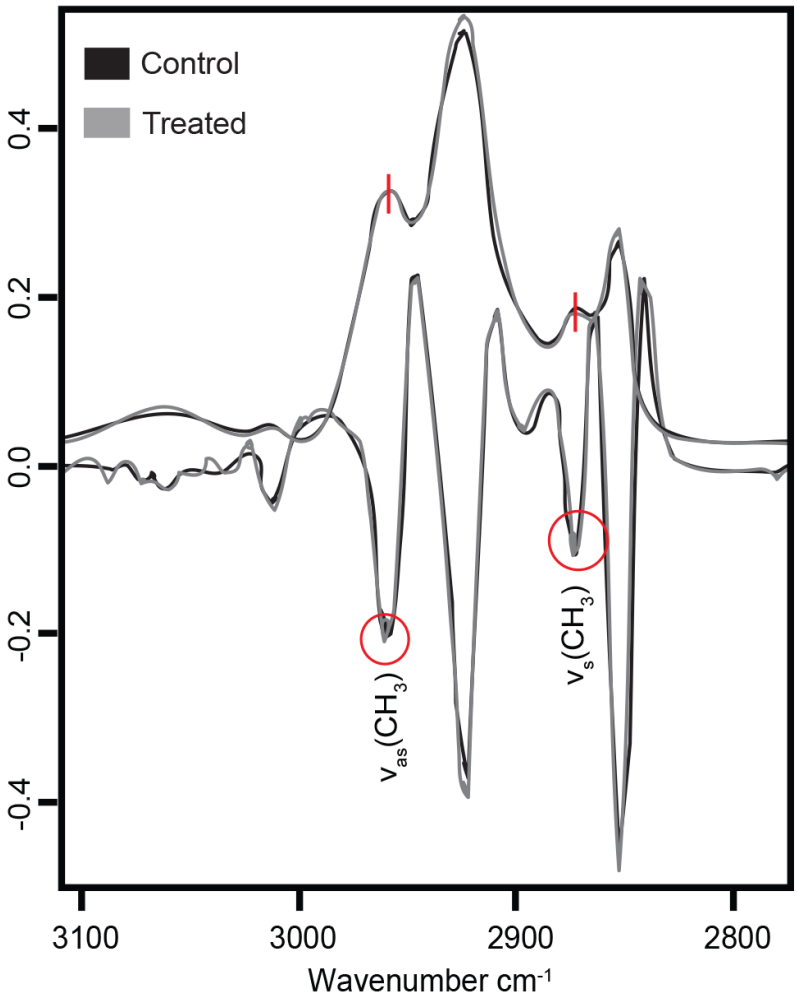

Figure 5.5.1 High wavenumber region of FT-IR spectra
FT-IR spectra of high wavenumber (top) accompanied by second derivative analysis (bottom). Areas of dissimilitude between control (black line) and Etn-treated (grey) samples are noted with a red notch on spectra and red circles on second derivative graph. Rubber band baseline corrected, and spectra normalized to Amide I n=32 scans/sample, N=3.

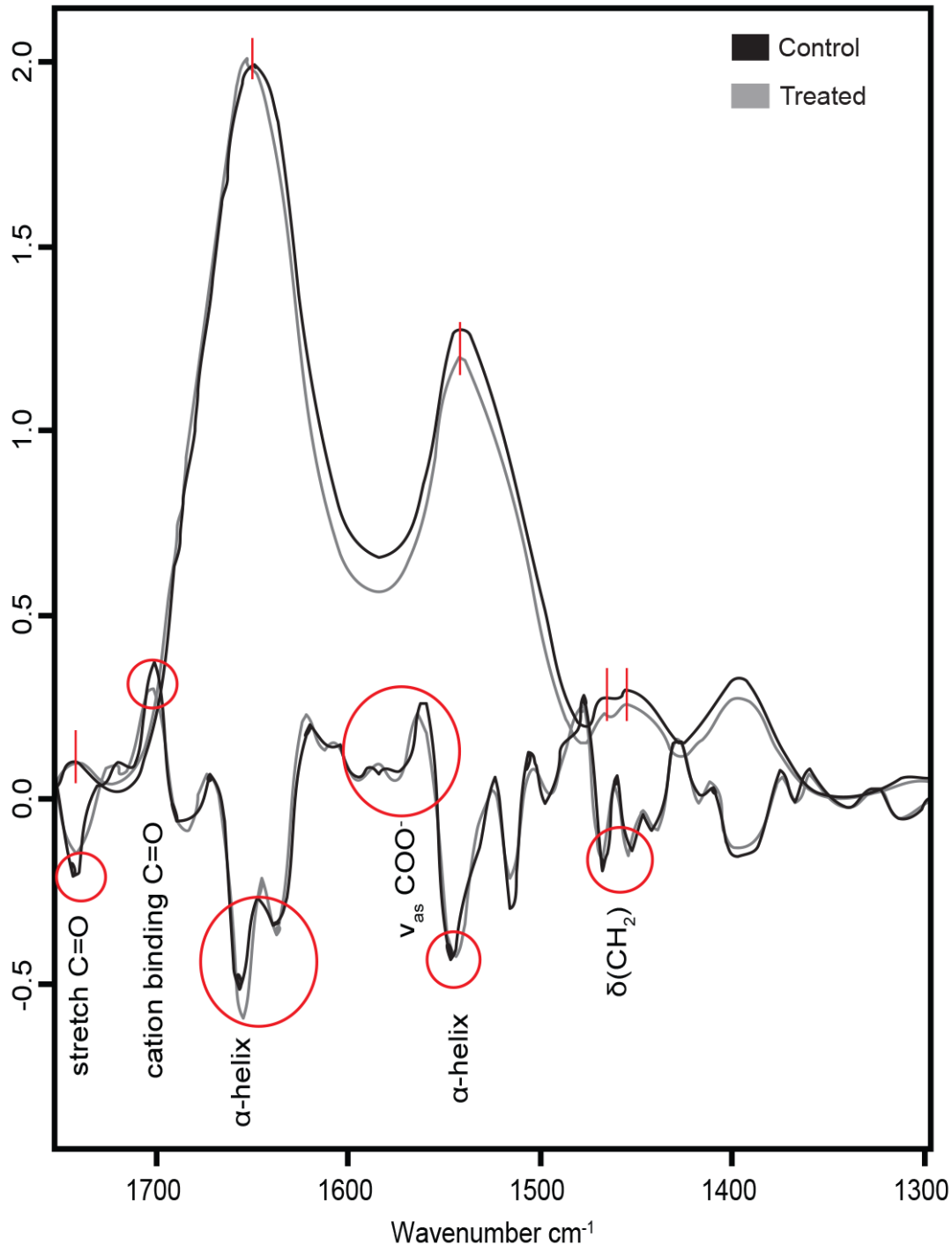

Figure 5.5.2 Mid wavenumber region FT-IR spectra
FT-IR spectra of mid-region wavenumber (top) accompanied by second derivative analysis (bottom). Areas of dissimilitude between control (black line) and Etn-treated (grey) samples are noted with a red notch on spectra and red circles on second derivative graph. Rubber band baseline corrected, and spectra normalized to Amide I n=32 scans/sample, N=3.

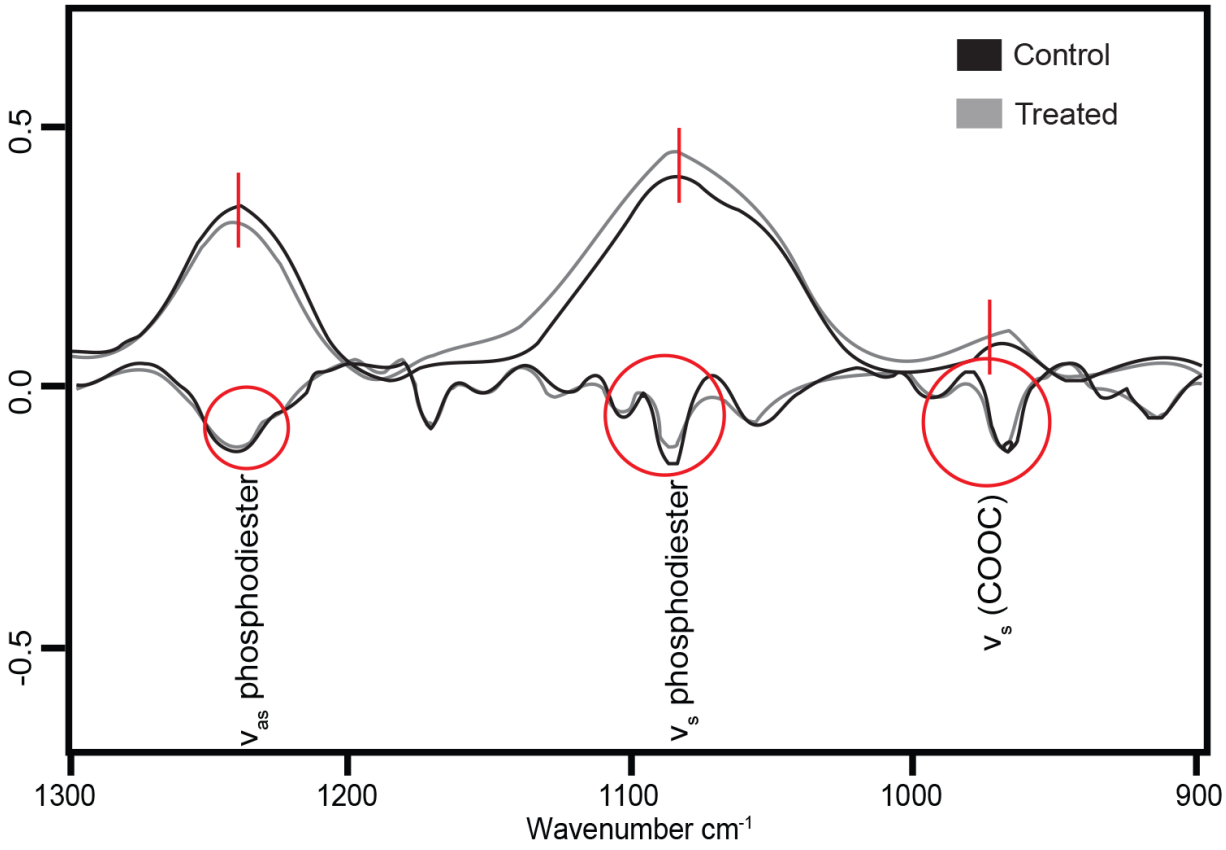

Figure 5.5.3 Low wavenumber region FT-IR spectra
FT-IR spectra of low wavenumber (top) accompanied by second derivative analysis (bottom). Areas of dissimilitude between control (black line) and Etn-treated (grey) samples are noted with a red notch on spectra and red circles on second derivative graph. Rubber band baseline corrected, and spectra normalized to Amide I n=32 scans/sample, N=3.

5.6 Discussion

FT-IR is a high resolution, high sensitivity technique that allows for the observation of vibrational patterns of polar bonds within a molecule. Moreover, this technique allows for the identification of subtle changes in these vibrational patterns due to treatment or experimental procedure when compared against a control. Changes in bond length, bond strength, participating atoms, or changes within the electronegativity of neighboring bonds can all influence the FT-IR spectra, making it one of the most sensitive classical techniques available to biochemists. Through computerized analysis of the resulting spectra, a second derivative graph can be created in order to more readily identify disruptions without the added step of attempting to deconvolute overlapping peaks.

High wavenumber regions of the mid-IR spectra care associated with vibrations of molecules. They include vibrations of C-H, N-H, S-H and O-H interactions. The predominant signatures seen are those of C-H interactions, with CH_3 and CH_2 symmetric and asymmetric vibrations being some of the predominant bands. These hydrocarbon bonds are mainly part of lipids, non-charged amino acid residues and fatty acid skeletons that help power and construct the cell. In the spectra taken from treated and untreated PC3 cells, there are four distinct peaks appearing in this region (~3100-2800 cm^{-1}, Figure 5.4.1).

Two peaks are associated with the asymmetric and vibrations of CH_3 and CH_2 (~2960 & ~2924 cm^{-1}), respectively, and the symmetric vibration of the same molecules (~2872 & ~2853 cm^{-1}). Symmetric and asymmetric vibrations refer to the direction in which the outer atoms move in respect to the central atom. In symmetric vibration, outer atoms pull in equal measure outwards before snapping back into their original conformation. In asymmetric vibration, the surrounding atoms move in different directions from the central atom, causing a disproportionate tilt towards

one of the bonds. Peak shifts at ~2960 and ~2872 cm^{-1} (Red notches on spectra and circles on 2nd derivative) represent changes in the symmetrical and asymmetrical vibration of CH_3 molecules, respectively, commonly associated to lipids. Experiments done on oils with varying degrees of saturation exhibited shifts of intensity in these methyl and methylene vibrations. More importantly, oils with higher amounts of saturated fatty acids tended to have a 1-2 downward wavenumber shift[65]. In Etn-treated cells, signal from symmetric and asymmetric methyl vibrations shifted upward in wavenumber compared to the control. With the knowledge that most FAs in cancer cells are saturated due to its lack of Δ 12 desaturase it could point towards the cell's need to import FAs from the extracellular environment due to shortage or degradation of intracellular stores.

Careful analysis of FT-IR spectra of the mid-range wavenumber region (~1700-1300 cm^{-1}) reveals changes in several vibration patterns. The first change seen is ~1743 cm^{-1}, a peak that corresponds to the carbonyl bond, C=O. This bond is commonly in phosphatidyl species (PC, PE, PS, in particular)[55]. This wavenumber shift is not surprising to find, as this lab has previously shown the change in phospholipid abundance, PE and PC, especially[19]. Another change in this region can be observed in the shift in wavenumber for the Amide I peak and subsequent changes amount the second derivative of that peak signal. The change observed at ~1650 cm^{-1} is linked to changes within the α-helix of the Amide I band. Additionally, three other peaks that are shifted under the Amide I and II bands are located on ~1705, ~1560, and ~1575 cm^{-1}.

The first of these signals corresponds to another carbonyl signal, commonly seen in molecules in which H-bonding creates affects cation binding. The other two bands seen downstream, ~1560 and ~1575 cm^{-1} correspond to the asymmetric vibration of the carboxyl groups of amino acid resides Asp and Glu that overlap under the Amide II signal. These two amino acids, as seen in Aim 2, are known to coordinate the sequestration of Ca^{2+} within the cell's ER reserves.

This change in wavenumber may be the effect of the ER stores emptying as a result of Etn treatment. The α-helix motif of the Amide II, seen around ~1548 cm^{-1} band is also shifted compared to the control. Finally, the last signal affected in the mid-wavenumber region corresponds to the scissoring of CH_2 outside of the vibrational plane of the central atom.

The low-wavenumber region of the mid-IR spectra (~1300-900 cm^{-1}) is often referred to as the fingerprint region of the FT-IR spectra due to the information about carbon skeleton bending[59]. It contains holds data pertaining to changes relating to nucleic acids and the phospholipid backbone. The peaks seen at ~1241 and ~1085 cm^{-1} are commonly associated with the asymmetric and symmetric phosphodiester bonds of nucleic acids, respectively. The ratio of these two bands in the control spectra is (Abs A/Abs B) is ~0.8, while the same ratio in treated cells is ~0.7. Taken together with the shift in peak at ~975 cm^{-1}, FT-IR analysis makes a case for the effect of Etn as an anticancer agent by not only disruption of lipids and proteins, but through the degradation of cell DNA.

FT-IR is an extremely sensitive technique that helps scientists visualize the vibrations of polar bonds shared by two or more atoms. Careful comparison between the spectra for control and Etn-treated cells came up with several differences in both the spectra and second derivative analysis. Due to the preliminary nature of this analysis, not all differences could be assigned to specific groups, apart from those vibrations already well-established in literature. Perhaps, the use of different FAs to change the composition of LDs, measuring spectra of cell fractions, rather than whole cells and the targeted restriction of the production of certain phospholipids could help identify specific peaks against a control. With this information, a library of spectra can be composed to use as a reference when screening compounds.

5.7 Conclusion

Previous Aims have given an insight on the fate of the content of the LDs in the cytoplasm of PC3 cells following lipolysis. Etn causes the disappearance of LDs in the cytoplasm through an increased rate of Ca^{2+}-mediated lipolysis, effectively inhibiting cells to maintain their fast-paced rate of growth and proliferation. Although these changes have been observed through validated methods in the previous experiments, it was of interest to probe whether there are observable differences in the cell's molecular makeup due to the action of Etn before the cells go into apoptotic phase. To make these observations, Etn-treated and control samples were measured through a highly sensitive, vibration-based technique known as FT-IR.

The field of evaluation of biological samples through FT-IR is fairly new. However, many strides have been made in the area, including the identification of key regions within the FT-IR spectra relating to specific macromolecules and the identification of vibrations and the most likely molecules they belong to. Within the breadth of this experiment, changes in the vibrational patterns of bonds relating to lipids, protein amino acid residues, protein conformations and nucleic acids were observed. Any divergence from the averaged spectra of multiple samples per group represent significant change in the molecular makeup of PC3 cells as a result of Etn treatment. While still in its preliminary stages of analysis, the sensitivity of this technique makes FT-IR a worthwhile tool to test the effectiveness of drugs in the future, following some standardization.

6 CONCLUSION AND FUTURE STUDIES

6.1 Summary and closing remarks

Cancer cells have developed several metabolic adaptations to ensure their survival and fuel their increased proliferation. Among these changes, the most notable are increased glucose through the Warburg effect and the creation of their own FAs through de novo lipogenesis. In so, lipid metabolism has been well characterized in cancer cells. Due to increased energy demands they rely on alternative routes of ATP generation, as is b oxidation. For this purpose, cancer cells have adapted to be able to take in FAs from the extracellular environment while also being able to create their own and store them in cytosolic reservoirs known as lipid droplets. These lipids can be used for energy, building blocks for cell membranes or signaling molecules. While most eukaryotic cells contain LDs they are not metabolically active, with the exception of adipocytes, hepatocytes, cancer cells and lactating breast tissue, and only have them as emergency reserves. This makes LDs an ideal target for anticancer compounds.

Etn is a small, polar molecule that serves as a precursor of the Kennedy pathway. Its downstream molecules are directly involved in the lipid metabolism of cells. While exogenous Etn treatment has been proven to induce apoptotic cell death, the full force of its effects on the lipid metabolism of prostate cancer cells have yet to be examined. Our studies have shown that on a gross, morphological level, Etn leads to a depletion of LDs in the cell cytoplasm as early as 1 hr following treatment and persisting to at least 16 hrs before surviving cell population recuperates (Aim 1). With this as a confirmation of change, the next step was to look at changes in signaling pathways.

Calcium is a ubiquitous second messenger within the cell and is involved in nearly all essential pathways. Ca^{2+} homeostasis is important for cell survival, as a dysregulation of $[Ca^{2+}]_i$ can have

disastrous effects in the cell. High $[Ca^{2+}]_i$ can induce cell lipolysis, atrophy genetic material, cause the depolarization of the mitochondrial membrane, and induce apoptosis. Here, we demonstrated for the first time that Etn activates calcium signaling mechanisms via the release of Ca^{2+} from intracellular stores. This transient increase in Ca^{2+} was seen in conditions were Ca^{2+} was and was not present in the extracellular environment, meaning that it's the intracellular reserves that is needed to begin the process of cell death. In tandem with the Ca^{2+} increase, there was an observable disruption of the mitochondria membrane potential, characterized by the hyperpolarization and subsequent depolarization of the mitochondria (Aim 2). This is especially relevant since it has been previously reported that a sustained depolarization of the mitochondria leads to leaking of Cytochrome c into the cytosol, making it impossible for ATP to be synthesized, and initiating cell death[40].

In addition to cell death, Ca^{2+} can be involved in the signaling pathway that induces the degradation of cytosolic lipid reserves. Ca^{2+} causes the activation of PKA through cAMP, leading to the hyperphosphorylation of perilipins on the LD surface. This changes the protein's conformation, allowing lipases, such as HSL to degrade the contents of the LDs. The contents inside the LDs are broken down in glycerol and free-FAs that excreted or processed by the cell in order to survive FA toxicity. Increased glycerol content in the media was seen as early as 1 hr following Etn treatment and was sustained until 16 hrs post-treatment, however, the effectiveness of Etn was attenuated with the use of Thapsigargin, a Ca^{2+} channel blocker. These results concur with the observation of LD reduction in the cell cytosol in Aim 1 and confirms the stimulation of lipolysis through a Ca^{2+}-mediated process (Aim 3).

Changes being undertaken as a response to Etn treatment are likely to have an effect on the molecular makeup of the cell due to the activation of survival and apoptotic pathways. Therefore,

it was important to determine these changes through high-resolution techniques. FT-IR is a classic vibration-based technique that causes movement through the excitation of bonds through IR energy. The resulting movement of polar bonds can be observed on the resulting spectra as a peak. Following Etn treatment wavenumber shifts and changes in band shape were observed in peaks pertaining lipids, nucleic acids and protein confirmation (Aim 4). Considering that Etn has been shown to induce apoptosis, lipolysis and the release of $[Ca^{2+}]_{i,}$ these results are not surprising. Although these results are preliminary, the observation of changes between control and Etn-treated samples makes FT-IR a valuable resource for drug development.

In closing, the hypothesis that the effectiveness of Etn was linked to lipid metabolism was correct. Etn is an anticancer drug that holds promise as a therapeutic. While traditional medication targets cell replication, Etn's effect on LDs make it an ideal candidate for treatment, as cancer cells are more likely to have metabolically active LDs that other normal tissue. Additionally, in previous studies with Etn done in the Aneja lab, it has been shown that Etn has a minimal effect on normal prostate tissue at the same concentrations in which it would be used as an anticancer therapeutic. Etn can be developed as an oral, non-toxic formulation that might reduce patient stress while providing faster, more targeted results against cancer.

6.2 Further studies

The mechanism of action of Etn within cancer cells must be completed in order to understand exactly why it works. Although Etn has been in use for several decades as a functional group for several drugs, how exactly the molecule gets into the cell has not been elucidated. Due to the short amount of time needed for Etn to cause an effect on cells following treatment, the possibility of specialized transporters or surface receptors is likely. Therefore, systematic evaluation of surface cell receptors involved in Ca^{2+} mediated processes through the use of blockers and agonists might be a good avenue to begin investigation. Alternatively, knockouts of membrane transporters could yield the answer to how Etn enters the cells. The answer to this question may be the missing piece of the therapeutic puzzle that might yield a new generation of targeted cancer treatments.

Additionally, the use of FT-IR in this work has demonstrated that it can detect minute changes within the molecular vibrations within cancer cells with a high degree of precision. Further than simply understanding that Etn treatment brought along molecular changes, it would be interesting to study the turnover of saturated versus unsaturated fatty acids within the cell. The use of standards, such as the addition of certain types of fatty acids bound to a transporter in the media could help define the shift of essential lipid-related peaks in order to make a quantitative comparison between experimental groups. Perhaps the fractionation of treated and control cells and separate analysis of different purified components could help eliminate some of the vibrational "noise" due to band overlap.

REFERENCES

[1] Group in *United States Cancer Statistics: 1999-2014 Incidence and Mortality Web-based Report*, *Vol.* Centers for Disease Control and Prevention and National Cancer Institute, Atlanta, **2017**.
[2] Siegel, et al., Cancer statistics, 2018. *CA Cancer J Clin* **2018**, *68*, 7-30.
[3] Jemal, et al., Global cancer statistics. *CA Cancer J Clin* **2011**, *61*, 69-90.
[4] Kroemer, et al., Classification of cell death: recommendations of the Nomenclature Committee on Cell Death 2009. *Cell death and differentiation* **2009**, *16*, 3-11.
[5] Galluzzi, et al., Molecular definitions of cell death subroutines: recommendations of the Nomenclature Committee on Cell Death 2012. *Cell Death and Differentiation* **2012**, *19*, 107-120.
[6] Evan, Proliferation, cell cycle and apoptosis in cancer. *Nature* **2001**, *411*, 7.
[7] de Boer-Dennert, Patient perceptions of the side-effects of chemotherapy: the influence of 5HT3 antagonists. *British Journal of Cancer* **1997**, *76*, 7.
[8] Luo, et al., Emerging roles of lipid metabolism in cancer metastasis. *Mol Cancer* **2017**, *16*, 76.
[9] Santos and Schulze, Lipid metabolism in cancer. *FEBS J* **2012**, *279*, 2610-2623.
[10] Baenke, et al., Hooked on fat: the role of lipid synthesis in cancer metabolism and tumour development. *Dis Model Mech* **2013**, *6*, 1353-1363.
[11] Sunami, et al., Lipid Metabolism and Lipid Droplets in Pancreatic Cancer and Stellate Cells. *Cancers (Basel)* **2017**, *10*.
[12] Guo, et al., Lipid droplets at a glance. *J Cell Sci* **2009**, *122*, 749-752.
[13] Kory, et al., Protein Crowding Is a Determinant of Lipid Droplet Protein Composition. *Dev Cell* **2015**, *34*, 351-363.
[14] Walther and Farese, The life of lipid droplets. *Biochim Biophys Acta* **2009**, *1791*, 459-466.
[15] Fujimoto and Parton, Not just fat: the structure and function of the lipid droplet. *Cold Spring Harb Perspect Biol* **2011**, *3*.
[16] Gomez de Cedron and Ramirez de Molina, Microtargeting cancer metabolism: opening new therapeutic windows based on lipid metabolism. *J Lipid Res* **2016**, *57*, 193-206.
[17] Lelliott and Vidal-Puig, Lipotoxicity, an imbalance between lipogenesis de novo and fatty acid oxidation. *Int J Obes Relat Metab Disord* **2004**, *28 Suppl 4*, S22-28.
[18] Liu, et al., Targeting lipid metabolism of cancer cells: A promising therapeutic strategy for cancer. *Cancer Lett* **2017**, *401*, 39-45.
[19] Saxena, et al., Preclinical Development of a Nontoxic Oral Formulation of Monoethanolamine, a Lipid Precursor, for Prostate Cancer Treatment. *Clin Cancer Res* **2017**, *23*, 3781-3793.
[20] Gibellini and Smith, The Kennedy pathway—De novo synthesis of phosphatidylethanolamine and phosphatidylcholine. *IUBMB Life* **2010**, *62*, 414-428.
[21] van Meer, et al., Membrane lipids: where they are and how they behave. *Nature Reviews Molecular Cell Biology* **2008**, *9*, 112.
[22] Ferreira, et al., Synthetic phosphoethanolamine has in vitro and in vivo anti-leukemia effects. *Br J Cancer* **2013**, *109*, 2819-2828.
[23] Devi, *Basic Histology: A Color Atlas & Text*, Jaypee Brothers,Medical Publishers Pvt. Limited, **2016**, p.

[24] Reid in *Characterization and Authentication of Cancer Cell Lines: An Overview*, (Ed. I. A. Cree), Humana Press, Totowa, NJ, **2011**, pp. 35-43.
[25] Kaighn, et al., Establishment and characterization of a human prostatic carcinoma cell line (PC-3). *Invest Urol* **1979**, *17*, 16-23.
[26] Mehlem, et al., Imaging of neutral lipids by oil red O for analyzing the metabolic status in health and disease. *Nat Protoc* **2013**, *8*, 1149-1154.
[27] Schneider, et al., NIH Image to ImageJ: 25 years of image analysis. *Nature Methods* **2012**, *9*, 671.
[28] Andersson, et al., PLD1 and ERK2 regulate cytosolic lipid droplet formation. *Journal of Cell Science* **2006**, *119*, 2246-2257.
[29] Clapham, Calcium Signaling. *Cell* **1995**, *80*, 10.
[30] Trump and Berezesky, Calcium-mediated cell injury and cell death. *The FASEB Journal* **1995**, *9*, 219-228.
[31] Murgia, et al., Controlling metabolism and cell death: at the heart of mitochondrial calcium signalling. *J Mol Cell Cardiol* **2009**, *46*, 781-788.
[32] McPhalen, et al., Calcium-binding sites in proteins: a structural perspective. *Adv Protein Chem* **1991**, *42*, 77-144.
[33] Allbritton, et al., Range of messenger action of calcium ion and inositol 1,4,5-trisphosphate. *Science* **1992**, *258*, 1812-1815.
[34] Berridge and Irvine, Inositol phosphates and cell signalling. *Nature* **1989**, *341*, 197-205.
[35] Catterall, Voltage-Gated Calcium Channels. *Cold Spring Harbor Perspectives in Biology* **2011**, *3*, a003947.
[36] Orrenius, et al., Regulation of cell death: the calcium–apoptosis link. *Nature Reviews Molecular Cell Biology* **2003**, *4*, 552.
[37] Perry, et al., Mitochondrial membrane potential probes and the proton gradient: a practical usage guide. *Biotechniques* **2011**, *50*, 98-115.
[38] Zoratti and Szabò, The mitochondrial permeability transition. *Biochimica et Biophysica Acta (BBA) - Reviews on Biomembranes* **1995**, *1241*, 139-176.
[39] Amuthan, Mitochondrial stress-induced calcium signaline, phenotypic changes and invasive behavior in human lung carcinoma A549 cells. *Oncogene* **2002**, *21*, 11.
[40] Heiskanen, Mitochondrial Depolarization Accompanies Cytochrome c Release During Apoptodid in PC6 Cells. *Journal of Biological Chemistry* **1999**, *274*, 5654-5658.
[41] Gunter, Conversion of esterified fura-2 and indo-1 to Ca2+-sensitive forms by mitochondria. *Am J Physiol* **1988**, *255*, 7.
[42] Scaduto, Measurement of Mitochondrial Membrane Potential Using Fluorescent Rhodamine Derivatives. *Biophysical Journal* **1999**, *76*, 9.
[43] Estes, et al., The role of action potentials in determining neuron-type-specific responses to nitric oxide. *Dev Neurobiol* **2015**, *75*, 435-451.
[44] Zaidi, et al., Lipogenesis and lipolysis: the pathways exploited by the cancer cells to acquire fatty acids. *Prog Lipid Res* **2013**, *52*, 585-589.
[45] Ray and Roy, Aberrant lipid metabolism in cancer cells - the role of oncolipid-activated signaling. *FEBS J* **2018**, *285*, 432-443.
[46] Mori, et al., The Tumor Microenvironment Modulates Choline and Lipid Metabolism. *Front Oncol* **2016**, *6*, 262.
[47] Allen and Beck, Role of calcium ion in hormone-stimulated lipolysis. *Biochem Pharmacol* **1986**, *35*, 767-772.

[48] Zangenberg, A dynamic in vitro lipolysis model: Controlling the rate of lipolysis by continuous addition of calcium. *European Journal of Pharmaceutical Scinces* **2001**, *14*, 115-122.
[49] Katocs, Role of Ca2+ in Adrenocortitropic Hormone-stimulated Lipolysis in the Perifused Fat Cell System. *J Biol Chem* **1974**, *249*, 6.
[50] Egan, et al., Mechanism of hormone-stimulated lipolysis in adipocytes: translocation of hormone-sensitive lipase to the lipid storage droplet. *Proceedings of the National Academy of Sciences* **1992**, *89*, 8537-8541.
[51] Thastrup, Thapsigargin, a tumor promoter, discharges intracellular Ca2+ stores by specific inhibition of the endoplasmic reticulum Ca2+-ATPase. *Proc Natl Acad Sci* **1990**, *87*, 5.
[52] Lytton, Thapsigargin Inhibits the Sarcoplasmic or Endoplasmic Reticulum Ca-ATPase Family of Calcium Pumps. *J Biol Chem* **1991**, *266*, 5.
[53] Fabian and Vogel in *Fourier Transform Infrared Spectroscopy of Calcium-Binding Proteins*, (Ed. H. J. Vogel), Springer New York, Totowa, NJ, **2002**, pp. 57-74.
[54] Barth, Infrared spectroscopy of proteins. *Biochim Biophys Acta* **2007**, *1767*, 1073-1101.
[55] Tamm, Infrared spectroscopy of proteins and peptides in lipid bilayers. *Quarterly Reviews of Biophysics* **1997**, *30*, 365-429.
[56] Andrew Chan and Kazarian, Attenuated total reflection Fourier-transform infrared (ATR-FTIR) imaging of tissues and live cells. *Chemical Society Reviews* **2016**, *45*, 1850-1864.
[57] Kazarian and Chan, ATR-FTIR spectroscopic imaging: recent advances and applications to biological systems. *Analyst* **2013**, *138*, 1940-1951.
[58] Kazarian and Chan, Applications of ATR-FTIR spectroscopic imaging to biomedical samples. *Biochimica et Biophysica Acta (BBA) - Biomembranes* **2006**, *1758*, 858-867.
[59] Derenne, et al., FTIR spectroscopy: a new valuable tool to classify the effects of polyphenolic compounds on cancer cells. *Biochim Biophys Acta* **2013**, *1832*, 46-56.
[60] Derenne, et al., Lipid quantification method using FTIR spectroscopy applied on cancer cell extracts. *Biochim Biophys Acta* **2014**, *1841*, 1200-1209.
[61] Baker, et al., Using Fourier transform IR spectroscopy to analyze biological materials. *Nature protocols* **2014**, *9*, 1771-1791.
[62] Georg, et al., Structural changes of sarcoplasmic reticulum Ca2+-ATPase upon Ca2+ binding studied by simultaneous measurement of infrared absorbance changes and changes of intrinsic protein fluorescence. *Biochimica et Biophysica Acta (BBA) - Bioenergetics* **1994**, *1188*, 139-150.
[63] Greenberg, et al., Perilipin, a major hormonally regulated adipocyte-specific phosphoprotein associated with the periphery of lipid storage droplets. *Journal of Biological Chemistry* **1991**, *266*, 11341-11346.
[64] Blanchette-Mackie, et al., Perilipin is located on the surface layer of intracellular lipid droplets in adipocytes. *Journal of Lipid Research* **1995**, *36*, 1211-1226.
[65] Christy and Egeberg, Quantitative determination of saturated and unsaturated fatty acids in edible oils by infrared spectroscopy and chemometrics. *Chemometrics and Intelligent Laboratory Systems* **2006**, *82*, 130-136.

APPENDIX

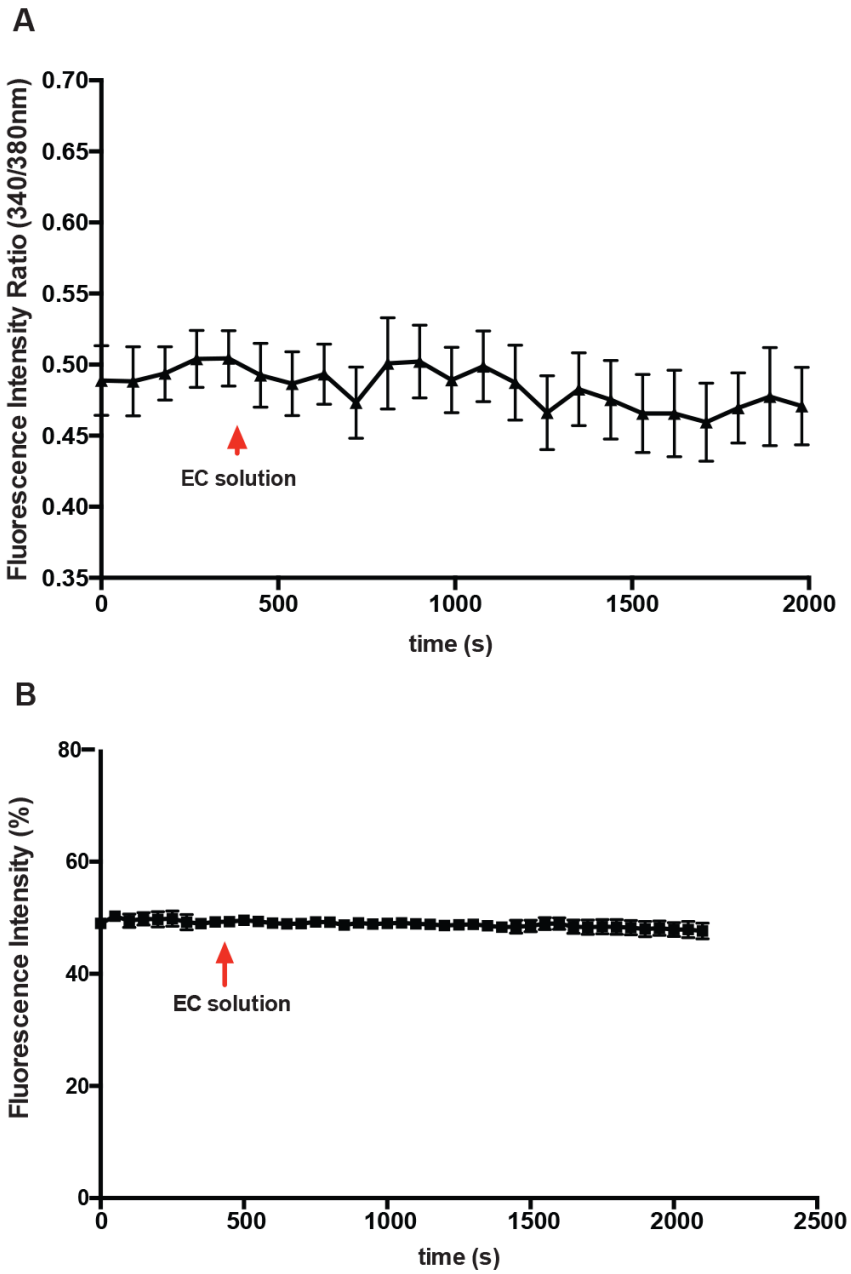

Figure A.1 Extracellular solutions controls for live imaging.
Control observations for calcium-dependent fluorescence in PC3 cells (A) and mitochondrial potential (B). Addition of blank extracellular solution marked by red arrow.

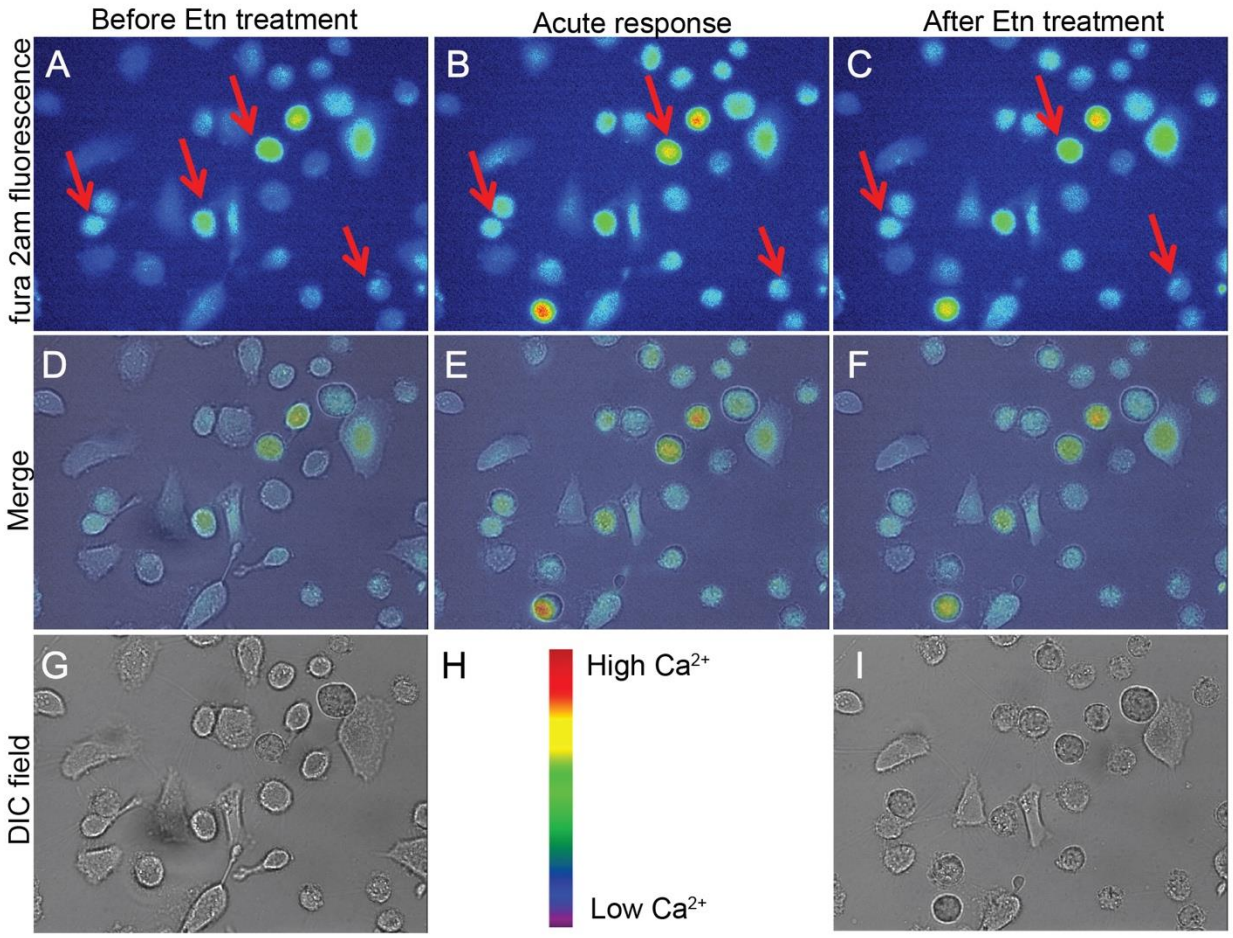

Figure A.2 Calcium-dependent fluorescent imaging of PC3 cells.
Fura-2am fluorescent ratio before, during and after Etn treatment (A-C) shows fluctuation of Ca^{2+} within the cell, according to fluorescent intensity (H). Images before and after treatment in brightfield are shown in G & I, and merged in D-F.

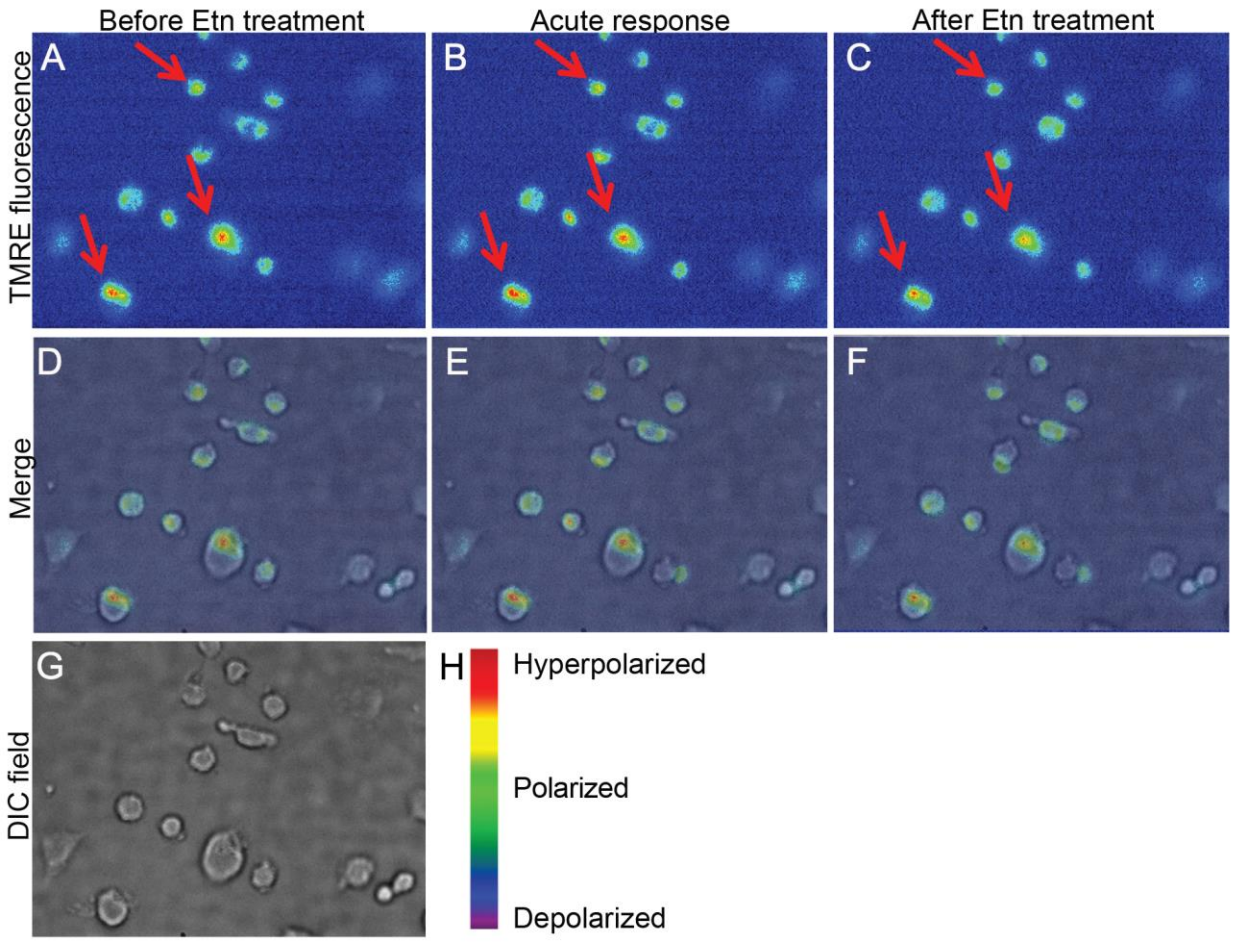

Figure A.3. Mitochondrial polarization-dependent fluorescent imaging of PC3 cells.
TMRE fluorescent imaging before, during and after Etn treatment (A-C) shows fluctuation of membrane potential in the mitochondria, according to fluorescent intensity (H). Images before and after treatment in brightfield are shown in G & I, and merged in D-F.